

---

# 1

---

## INTRODUCTION

This text concerns the analysis of transmission-line structures that serve to guide electromagnetic (EM) waves between two or more points. The analysis of transmission lines consisting of two parallel conductors of uniform cross section has traditionally been a fundamental subject in electrical engineering (EE) [A.1,A.3,A.6]. Prior to the introduction of digital computer engineering topics into the undergraduate EE curricula, all EE undergraduates were required to complete a course on two-conductor transmission lines. However, because of the introduction of computer engineering courses into an already crowded 4-year undergraduate degree program, the transmission-line course in many EE programs has been relegated to a senior technical elective if offered at all. Unfortunately, the increasing use of high-speed digital technology requires that all EE undergraduates must have a working knowledge of transmission lines. In addition, the use of multiconductor transmission lines (MTLs) consisting of more than two conductors is becoming more widespread because of the increasing need for high-volume and high-speed data and signal transmission. Signal integrity, the effect of the transmission line on the signal transmission, is becoming a critical aspect of high-speed digital system performance.

This text is the second edition of a previous text concerning the analysis of MTLs. It has been reorganized with the emphasis given toward a university textbook for a senior/graduate textbook on transmission lines. The text has been reorganized so that each broad analysis topic, for example, per-unit-length parameters, frequency-domain analysis, time-domain analysis, incident field excitation, and transmission-line networks, has a chapter concerning two-conductor lines followed immediately by

a chapter on MTLs for that topic. This allows the instructors to choose their emphasis either on two-conductor lines or on MTLs, or on both. This organization also makes it easier for the reader to understand the analysis of MTLs. The analysis of MTLs is very similar to that of two-conductor lines except that the detail is considerably increased. However, with the aid of matrix symbology and techniques most of the MTL topics are straightforward extensions of the corresponding two-conductor line topics. Hence by devoting a separate chapter to each two-conductor line topic and then following that with a chapter on the corresponding MTL topic, the MTL material can be more readily understood.

The analysis of MTLs is somewhat more difficult than the analysis of two-conductor lines, but the applications cover a broad frequency spectrum and encompass a wide variety of transmission lines ranging from power transmission lines to microwave circuits [B.4, Refs. 1–16]. However, matrix methods and notation provide a straightforward extension of many, if not most, of the aspects of two-conductor lines to MTLs. Many of the concepts and performance measures of two-conductor lines require more elaborate concepts when extended to MTLs. For example, in order to eliminate reflections at terminations on a two-conductor line, we simply terminate it in a matched load, that is, a load resistance that equals the (real) characteristic impedance of the line. In the case of MTLs, we must terminate the line in a *characteristic impedance matrix* or network of resistances in order to eliminate all reflections. It is not sufficient to simply insert a resistance between each conductor and the reference conductor; there must also be resistances between every pair of conductors. In order to describe the degree of mismatch of a particular load impedance on a two-conductor line, we compute a scalar reflection coefficient. In the case of an MTL, we can obtain the analogous quantity, but it becomes a *reflection coefficient matrix*.

On a two-conductor line there is a forward- and a backward-traveling wave each traveling in opposite directions with velocity  $v$ . In the case of an MTL consisting of  $n + 1$  conductors, there exist  $n$  forward- and  $n$  backward-traveling waves each with its own velocity. Each pair of forward- and backward-traveling waves is referred to as a *mode*. If the MTL is immersed in a homogeneous medium, each mode velocity is identical to the phase velocity of light in that medium. The mode velocities of an MTL that is immersed in an inhomogeneous medium (such as wires with dielectric insulations or printed circuit boards (PCBs)) will, in general, be different.

The governing transmission-line equations for a two-conductor line will be a coupled set of two first-order partial differential equations for the line voltage  $V(z, t)$  and line current  $I(z, t)$ , where the line conductors are parallel to the  $z$  axis and time is denoted as  $t$ . In the case of an MTL consisting of  $n + 1$  conductors parallel to the  $z$  axis, the corresponding governing equations are a coupled set of  $2n$  first-order *matrix* partial differential equations relating the  $n$  line voltages  $V_i(z, t)$  and  $n$  line currents  $I_i(z, t)$  for  $i = 1, 2, \dots, n$ . The number of conductors may be quite large, for example,  $n + 1 = 100$ , in which case efficiency of solution of the  $2n$  MTL equations becomes an important consideration. The ease of solution of the MTL equations depends upon the assumptions or approximations one is willing to make about the line, for example, uniform line versus nonuniform line, lossless line versus lossy line, a homogeneous

surrounding medium versus an inhomogeneous surrounding media, and so on, as well as the solution technique chosen. Although it is tempting to dismiss the analysis of MTLs as simply being a special case of two-conductor lines and thereby not requiring scrutiny, this is not the case. In addition to a thorough discussion of two-conductor lines, we will examine the methods for solution of MTLs. Numerous experimental results will be compared to the predictions of the transmission-line equations, for both two-conductor lines and MTLs, in order to show their accuracy as well as the relative influence of the line parameters.

The analysis of an MTL for the resulting  $n$  line voltages  $V_i(z, t)$  and  $n$  line currents  $I_i(z, t)$  is in general, a three-step process:

**Step 1:** *Determine the per-unit-length parameters of inductance, capacitance, conductance, and resistance for the given line.* All cross-sectional information about the particular line such as conductor cross sections, wire radii, conductor separations, and so on that distinguishes it from some other line is contained in these per-unit-length parameters and nowhere else. In the case of an two-conductor line, these parameters are scalars. In the case of an MTL consisting of  $n + 1$  conductors, these parameters are contained in matrices that are of dimension  $n \times n$ . The MTL equations are identical in form for all lines: only the per-unit-length parameters are different. Without the determination of the per-unit-length parameters for the specific line, one cannot solve the resulting MTL equations because the coefficients in those equations (the per-unit-length parameters) will be unknown.

**Step 2:** *Determine the general solution of the resulting MTL equations.* For a two-conductor line, the general solution consists of the sum of a forward- and a backward-traveling wave. In the case where the sources driving the line are general excitation waveforms, these waves are represented by *two unknown functions* that are functions of position along the line  $z$  and time  $t$ . In the case of sinusoidal steady-state excitation of the line, there are *two complex-valued undetermined constants*. For an MTL consisting of  $n + 1$  conductors, the general solution consists of the sum of  $n$  forward- and  $n$  backward-traveling waves. In the case where the sources driving the line are general excitation waveforms, these waves are represented by *2n unknown functions* that are functions of position along the line  $z$  and time  $t$ . In the case of sinusoidal steady-state excitation of the line, there are *2n complex-valued undetermined constants*.

**Step 3:** *Incorporate the terminal conditions to determine the unknown functions or unknown coefficients in the general form of the solution.* A transmission line will have terminations at the left and right ends consisting of independent voltage and/or current sources and lumped elements such as resistors, capacitors, inductors, diodes, transistors, and so on. These *terminal constraints* provide the additional  $2n$  equations ( $n$  for the left termination and  $n$  for the right termination), which can be used to explicitly determine the  $2n$  undetermined functions or the  $2n$  coefficients in the general form of the MTL equation solution that was obtained in step 2.

The above sequence of steps is referred to as the *direct method*. There are also other methods of solution that avoid these individual steps. These are *numerical* methods that seek to directly integrate the transmission-line differential equations and at the same time include the terminal constraint relations at the two ends of the line. An example of such a method that we will investigate is the finite-difference, time-domain (FDTD) method.

The excitation sources for the MTL will have several forms. Independent lumped sources within the two termination networks are one method of exciting the line. Each source is intended to be coupled to the endpoint of the line to which it is attached. However, the electromagnetic fields associated with the current and voltage on that line interact with neighboring lines inducing signals at those endpoints. This coupling is *unintentional* and is referred to as *crossstalk*. Another method of exciting a line is with an incident electromagnetic field such as radio, radar, or TV signals, or a lightning pulse. This form of unintended excitation produces sources that are distributed along the line and will also induce unintentional signals at the line endpoints that may cause *interference*. Lumped sources can occur at discrete points along the line as with the direct attachment of a lightning stroke. The effect of incident fields distributed either along the line or at discrete points can be included in the MTL equations. In order to obtain the complete solution for the line voltages and currents via the direct solution method, *each of the above three steps must be performed* and in the above order. Throughout our discussions, this sequence of solution steps should be kept in mind.

Electromagnetic fields are, in reality, distributed throughout space. If a structure's largest dimension is electrically small, that is, much less than a wavelength, we can approximately lump the EM effects into circuit elements as in lumped-circuit theory and represent the line with a lumped equivalent circuit, thereby avoiding a direct solution of the transmission-line equations. The transmission-line formulation that we will use to analyze the line views the line as a distributed-parameter structure along the line axis and thereby extends the lumped-circuit analysis techniques to structures that are electrically large in this dimension. However, the cross-sectional dimensions, for example, conductor separations, must be electrically small in order for the analysis to yield valid results. The fundamental assumption for all transmission-line formulations and analyses whether it be for a two-conductor line or an MTL is that the electromagnetic field surrounding the conductors has a transverse electromagnetic (TEM) structure. A TEM field structure is one in which the electric and magnetic fields in the space surrounding the line conductors are transverse or perpendicular to the line axis. In other words, the TEM field structure has no components of the electric or magnetic fields directed along the line axis. The electric and magnetic fields in the space around the line conductors propagate along the line as waves and are said to propagate in the TEM mode. One of the important consequences of the TEM mode of propagation is to allow the unique definition of line voltages and currents. Voltage and current are normally definable only for dc or static fields [A.1]. For the TEM field structure, voltage between the line conductors and currents flowing on those conductors can be uniquely defined even though the fields are varying with time. There are certain nonideal aspects of an MTL, such as imperfect line conductors and/or an inhomogeneous surrounding medium, that, theoretically, invalidate the

TEM mode, transmission-line equation description. However, we will include these nonideal properties in the transmission-line equation formulation of the ideal TEM mode on the assumption that their effects are small. This is referred to as the quasi-TEM mode assumption. In addition to the TEM mode of propagation, there may exist other higher order modes of propagation [17–19]. These higher order modes generally have cutoff frequencies below which they are highly attenuated and for all practical purposes do not propagate. The TEM mode has a cutoff frequency of dc. For typical transmission-line structures such as cables and PCBs, the higher order modes are cutoff (or highly attenuated) for frequencies up to the lower gigahertz frequency range. Consequently using the TEM mode, transmission-line equation formulation to analyze typical lines will provide an accurate analysis of the line for frequencies of excitation well into the lower gigahertz frequency range. An important consequence of the TEM mode, MTL equation formulation is that the sum of the line currents at any cross section of the line is zero. In this sense we say that one of the conductors, the *reference conductor*, is the return for the other  $n$  currents. Even though the line cross section is electrically small, it may not be true that the currents sum to zero at any cross section; there may be other currents in existence on the line conductors [20–23]. Presence of nearby conductors or other metallic structures that are not included in the formulation may cause these additional currents [24]. Asymmetries in the physical terminal excitation such as offset source positions (which are implicitly ignored in the terminal representation) can also create these non-TEM currents [24]. It is important to understand these restrictions on the applicability of the transmission-line equation representation and the validity of the results obtained from it.

Although there is a voluminous base of references for this topic, important ones will be referenced, where appropriate, by [x]. These are grouped into two categories—those by the author (grouped by category) and other references. References consisting of publications on this topic by the author are listed at the end of the text and are grouped by category. Additional references will be listed at the end of each chapter.

## 1.1 EXAMPLES OF MULTICONDUCTOR TRANSMISSION-LINE STRUCTURES

There are a number of examples of wave-guiding structures that may be viewed as “transmission lines.” Figure 1.1 shows examples of  $(n + 1)$ -conductor, wire-type lines consisting of parallel wires. Throughout this text, we will refer to conductors that have circular–cylindrical cross sections as *wires*. The conductors are parallel to the line axis, which is the  $z$  axis of a rectangular coordinate system. One of the conductors is designated as the 0 (zero) conductor or *reference conductor*. The line voltages  $V_i(z, t)$  are defined between each of the other  $n$  conductors and this reference conductor. The currents flowing on the other  $n$  conductors,  $I_i(z, t)$ , “return” along this reference conductor. The voltages and currents are functions of position along the line,  $z$ , and time  $t$ . Figure 1.1(a) shows an example of  $n + 1$  wires, where the reference conductor is another wire. Typical examples of such lines are ribbon

cables used to interconnect electronic systems. Figure 1.1(b) shows  $n$  wires above an infinite, perfectly conducting ground plane (the reference conductor). Typical examples are cables that have a metallic structure as a return or high-voltage power distribution lines. Figure 1.1(c) shows  $n$  wires within an overall cylindrical shield (the reference conductor). Shields are often placed around groups of wires in order to prevent or reduce the coupling of electromagnetic fields to the wires from adjacent wires (crosstalk) or from distant sources such as radar transmitters or radio and television transmitters. Normally, all wires are surrounded by circular–cylindrical dielectric insulations. However, these insulations are omitted from these figures and, in some cases, may be ignored in the analysis of such lines. Hence the surrounding medium is said to be *homogeneous* in that the permittivity  $\epsilon$  and permeability  $\mu$  of the surrounding dielectric medium are constants and are independent of position. Hence, the wire structures of Figure 1.1 are said to constitute lines in a *homogeneous medium*. For the lines in Figure 1.1(a) and (b), the only logical homogeneous medium of infinite extent would be free space with parameters of *permittivity*  $\epsilon_0$  and *permeability*  $\mu_0$ . For the line within an overall shield in Figure 1.1(c), the fields are contained within the shield that may be a homogeneous dielectric other than free space with parameters  $\epsilon = \epsilon_r \epsilon_0$  and  $\mu = \mu_0$ . The permeability of all dielectrics is that of free space, whereas the permittivity is characterized by a relative permittivity (relative to that of free space) of  $\epsilon_r$ . Thus dielectrics affect electric fields and do not affect magnetic fields. The wires in each of these structures are also shown as being of *uniform cross section* along their length and parallel to each other (as well as the

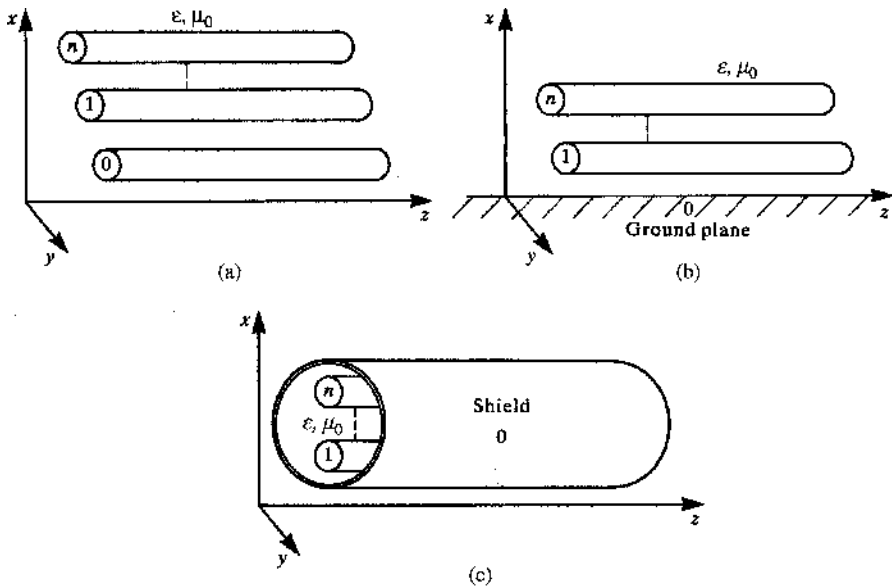


**FIGURE 1.1** Multiconductor lines in homogeneous media: (a)  $(n + 1)$ -wire line, (b)  $n$  wires above a ground plane, and (c)  $n$  wires within a cylindrical shield.

ground plane in Fig. 1.1(b) and the shield axis in Fig. 1.1(c)). Such lines are said to be *uniform lines*. Nonuniform lines in which the conductors either are not of uniform cross section along their length or are not parallel arise from either nonintentional or intentional reasons. For example, the conductors of a high-voltage power distribution line, because of their weight, sag and are not parallel to the ground. Tapered lines are intentionally designed to give certain desirable characteristics in microwave filters.

Figure 1.2 shows examples of lines wherein the conductors have rectangular cross sections. Figure 1.2(a) shows a structure having  $n$  conductors of rectangular cross

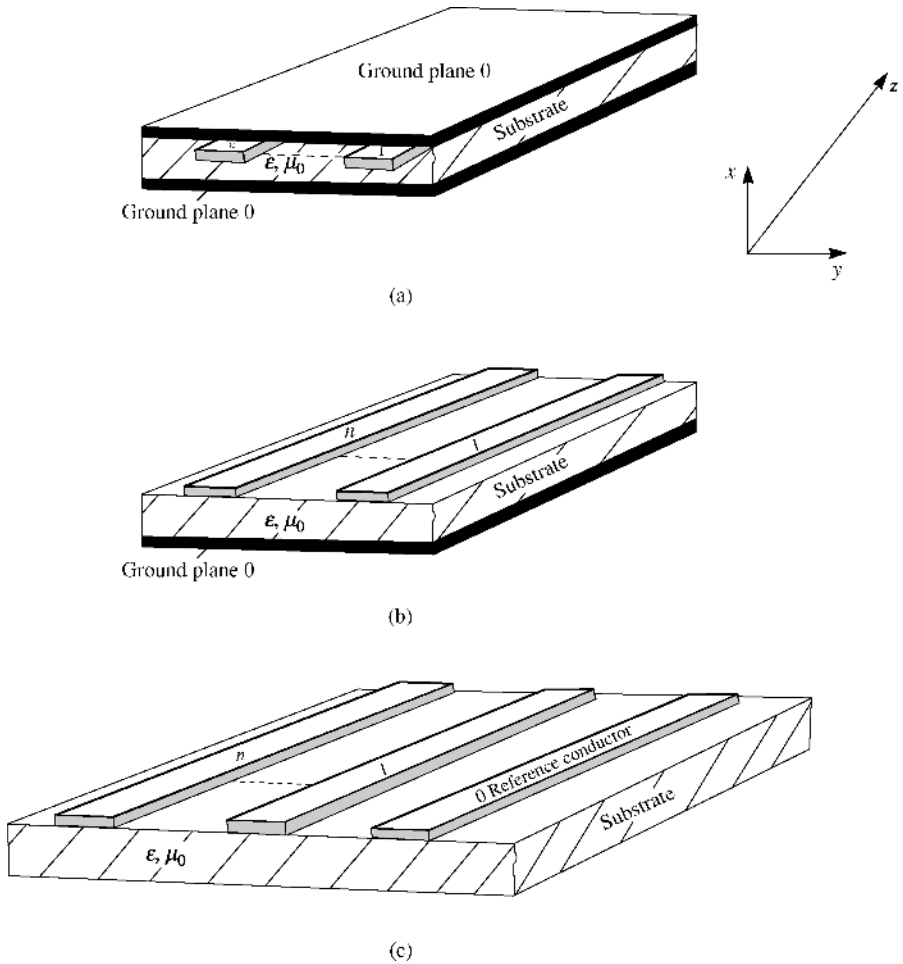


**FIGURE 1.2** Multiconductor lines consisting of conductors of rectangular cross section (lands): (a) an  $n$ -conductor coupled stripline (homogeneous medium), (b) an  $n$ -conductor coupled microstrip line (inhomogeneous medium), and (c)  $n$  lands on a PCB (inhomogeneous medium).

section (*lands*) imbedded in a dielectric substrate. This type of structure is referred to as a *coupled stripline*. Infinite ground planes are on either side of the substrate and constitute the reference conductor(s). This structure represents the case of innerplanes in PCBs. Multiple layers of interconnected lands are buried in a single board and allow for “wiring” the board without taking up a large surface area. “Vias” connect lands on each level. Figure 1.2(b) shows  $n$  lands on one side of a dielectric substrate and an infinite ground plane, the reference conductor, on the other side. This is referred to in microwave literature as a *coupled microstrip* and is used to construct microwave filters. This structure also represents the outer layer of a printed circuit board that has innerplanes. Figure 1.2(c) shows  $n + 1$  lands on one side of the dielectric substrate. One of those lands constitutes the reference conductor to which all the other line voltages are referenced. This type of structure is common on PCBs in low-cost electronic circuits that do not contain innerplanes. The stripline of Figure 1.2(a) has the fields contained between the two ground planes much like the shielded cable of Figure 1.1(c). Hence, the dielectric is homogeneous with permittivity  $\varepsilon = \varepsilon_r \varepsilon_0$  and permeability  $\mu = \mu_0$ . The structures of Figure 1.2(b) and (c) constitute lines in an inhomogeneous medium in that the electric field lines will exist partly in the substrate and partly in the surrounding air.

The structures in Figure 1.1, as well as the coupled stripline in Figure 1.2(a), are, by implication, immersed in a homogeneous medium. Therefore, the velocity of propagation of the waves on those lines is equal to that of the medium in which they are immersed or  $v = 1/\sqrt{\mu\varepsilon}$ , where  $\mu$  is the *permeability* of the surrounding medium and  $\varepsilon$  is the *permittivity* of the surrounding medium. For free space, these become  $\mu_0 = 4\pi \times 10^{-7}$  H/m and  $\varepsilon_0 \cong 1/36\pi \times 10^{-9}$  F/m. The velocity of propagation in free space is  $v_0 = 1/\sqrt{\mu_0\varepsilon_0} = 2.99792458 \times 10^8$  m/s. For the structures shown in Figure 1.2(b) and (c), which are immersed in an *inhomogeneous medium* (the fields exist partly in free space and partly in the substrate), there are  $n$  waves or *modes* whose velocities are, in general, different. This complicates the analysis of such structures as we will see.

## 1.2 PROPERTIES OF THE TEM MODE OF PROPAGATION

As mentioned previously, the fundamental assumption in any transmission-line formulation is that the electric field intensity vector  $\mathcal{E}(x, y, z, t)$  and the magnetic field intensity vector  $\mathcal{H}(x, y, z, t)$  satisfy the TEM field structure, that is, they lie in a plane (the  $x$ - $y$  plane) transverse or perpendicular to the line axis (the  $z$  axis). Therefore, it is appropriate to examine the general properties of this TEM mode of propagation or field structure.

Consider a rectangular coordinate system shown in Figure 1.3 illustrating a propagating TEM wave in which the field vectors are assumed to lie in a plane (the  $x$ - $y$  plane) that is transverse to the direction of propagation (the  $z$  axis). These field vectors are denoted with a  $t$  subscript to denote that they lie in the *transverse* ( $x$ - $y$ ) plane. It is assumed that the medium is homogeneous, linear, and isotropic and is characterized by the scalar parameters of permittivity  $\varepsilon$ , permeability  $\mu$ , and conductivity  $\sigma$ .

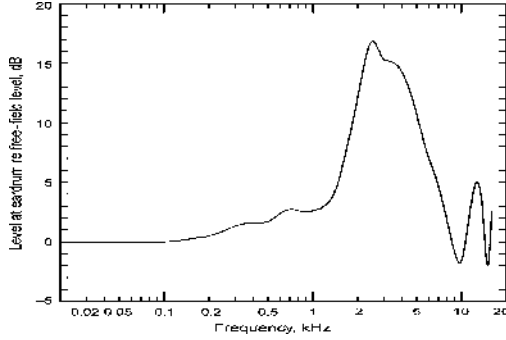


**FIGURE 1.3** Illustration of the electromagnetic field structure of the TEM mode of propagation.

Maxwell's equations in differential or point form are [A.1,A.3,A.6]:

$$\nabla \times \vec{\mathcal{E}}_t = -\mu \frac{\partial \vec{\mathcal{H}}_t}{\partial t} \quad (1.1a)$$

$$\nabla \times \vec{\mathcal{H}}_t = \sigma \vec{\mathcal{E}}_t + \varepsilon \frac{\partial \vec{\mathcal{E}}_t}{\partial t} \quad (1.1b)$$

Equation (1.1a) is Faraday's law, and Eq. (1.1b) is Ampere's law. The del operator  $\nabla$  can be broken into two components: one component,  $\nabla_z$ , in the  $z$  direction and the other component,  $\nabla_t$ , in the transverse plane, as in [A.1]

$$\nabla = \nabla_t + \nabla_z \quad (1.2a)$$

where

$$\nabla_t = \vec{a}_x \frac{\partial}{\partial x} + \vec{a}_y \frac{\partial}{\partial y} \quad (1.2b)$$

$$\nabla_z = \vec{a}_z \frac{\partial}{\partial z} \quad (1.2c)$$

and  $\vec{a}_x$ ,  $\vec{a}_y$ , and  $\vec{a}_z$  are unit vectors pointing in the appropriate directions. Applying (1.2) to (1.1) gives

$$(\nabla_t + \nabla_z) \times \vec{\mathcal{E}}_t = \underbrace{\nabla_t \times \vec{\mathcal{E}}_t}_{z \text{ directed}} + \underbrace{\nabla_z \times \vec{\mathcal{E}}_t}_{\text{in the transverse plane}} = -\mu \frac{\partial \vec{\mathcal{H}}_t}{\partial t} \quad (1.3a)$$

$$(\nabla_t + \nabla_z) \times \vec{\mathcal{H}}_t = \underbrace{\nabla_t \times \vec{\mathcal{H}}_t}_{z \text{ directed}} + \underbrace{\nabla_z \times \vec{\mathcal{H}}_t}_{\text{in the transverse plane}} = \sigma \vec{\mathcal{E}}_t + \varepsilon \frac{\partial \vec{\mathcal{E}}_t}{\partial t} \quad (1.3b)$$

Matching those components on both sides of (1.3) in the  $z$  direction and in the transverse plane gives

$$\vec{a}_z \times \frac{\partial \vec{\mathcal{E}}_t}{\partial z} = -\mu \frac{\partial \vec{\mathcal{H}}_t}{\partial t} \quad (1.4a)$$

$$\vec{a}_z \times \frac{\partial \vec{\mathcal{H}}_t}{\partial z} = \sigma \vec{\mathcal{E}}_t + \varepsilon \frac{\partial \vec{\mathcal{E}}_t}{\partial t} \quad (1.4b)$$

$$\nabla_t \times \vec{\mathcal{E}}_t = 0 \quad (1.4c)$$

$$\nabla_t \times \vec{\mathcal{H}}_t = 0 \quad (1.4d)$$

Equations (1.4a) and (1.4b) show that the electric and magnetic field intensity vectors are orthogonal (perpendicular to each other) [A.1]. Equations (1.4c) and (1.4d) are identical in the transverse plane to those for *static fields* [A.1]. This shows that the electric and magnetic fields of a TEM field distribution satisfy a static distribution in the transverse plane. In other words, the electric and magnetic fields in the transverse plane are identical in structure to those for dc excitation, even though they vary with time. This is an extremely important consequence of the TEM field structure in that (a) voltages and currents that are ordinarily definable only for static (dc) excitation can be uniquely defined for this problem in the transverse plane even though the fields are time varying, and (b) we can determine important transmission-line parameters such as per-unit-length capacitance, inductance, and conductance by using only static field analysis methods in the transverse ( $x$ - $y$ ) plane, which greatly simplifies their determination.

An important vector identity is that the curl of the gradient of some scalar field  $f(x, y, z)$  is always zero:  $\nabla \times \nabla f(x, y, z) = 0$  [A.1]. In the transverse plane, this identity translates to

$$\nabla_t \times \nabla_t f(x, y) = 0 \quad (1.5)$$

where  $\nabla_t$  is the transverse del operator given in (1.2b). Because of (1.4c), (1.4d), and this identity, we may define each of the transverse field vectors as the transverse gradients of some auxiliary scalar fields or *potential functions*,  $\phi(x, y)$  and  $\psi(x, y)$ ,

which lie in the transverse plane as [A.1]

$$\vec{\mathcal{E}}_t = e(z, t)\nabla_t\phi(x, y) \quad (1.6a)$$

$$\vec{\mathcal{H}}_t = h(z, t)\nabla_t\psi(x, y) \quad (1.6b)$$

Note that the field vectors are separable into the product of functions of  $z$  and  $t$  and functions of the transverse plane coordinates  $x$  and  $y$ . This is permissible in the rectangular coordinate system [A.1]. Because the transverse electric and magnetic field vectors are orthogonal, according to (1.6) the gradient fields  $\nabla_t\phi(x, y)$  and  $\nabla_t\psi(x, y)$  are also orthogonal in the transverse plane. Hence, the scalar field lines for  $\phi = \text{constant}$  are everywhere in the transverse plane orthogonal to the scalar field lines for  $\psi = \text{constant}$ . Gauss' laws in the transverse plane become [A.1]

$$\nabla_t \cdot \vec{\mathcal{E}}_t = 0 \quad (1.7a)$$

$$\nabla_t \cdot \vec{\mathcal{H}}_t = 0 \quad (1.7b)$$

Applying (1.7) to (1.6) gives

$$\nabla_t \cdot \nabla_t\phi(x, y) = \nabla_t^2\phi(x, y) = 0 \quad (1.8a)$$

$$\nabla_t \cdot \nabla_t\psi(x, y) = \nabla_t^2\psi(x, y) = 0 \quad (1.8b)$$

where

$$\nabla_t^2\phi(x, y) = \frac{\partial^2\phi(x, y)}{\partial x^2} + \frac{\partial^2\phi(x, y)}{\partial y^2} = 0 \quad (1.9a)$$

$$\nabla_t^2\psi(x, y) = \frac{\partial^2\psi(x, y)}{\partial x^2} + \frac{\partial^2\psi(x, y)}{\partial y^2} = 0 \quad (1.9b)$$

are Laplace's equations in the transverse plane [A.1]. Equations (1.9) show that the auxiliary scalar potential functions satisfy Laplace's equation in any transverse plane, as is the case for static (dc) fields. This again shows that the electric and magnetic field structure in the transverse plane for the TEM mode of propagation is identical to that of a static (dc) distribution. As we will show later, there are numerous static field methods to compute this static field distribution.

Now suppose we take the cross product of the  $z$ -directed unit vector with (1.4a) and (1.4b). This gives

$$\vec{a}_z \times \left[ \vec{a}_z \times \frac{\partial \vec{\mathcal{E}}_t}{\partial z} \right] = -\mu \left[ \vec{a}_z \times \frac{\partial \vec{\mathcal{H}}_t}{\partial t} \right] \quad (1.10a)$$

$$\vec{a}_z \times \left[ \vec{a}_z \times \frac{\partial \vec{\mathcal{H}}_t}{\partial z} \right] = \sigma(\vec{a}_z \times \vec{\mathcal{E}}_t) + \varepsilon \left[ \vec{a}_z \times \frac{\partial \vec{\mathcal{E}}_t}{\partial t} \right] \quad (1.10b)$$

However,

$$\vec{a}_z \times \left[ \vec{a}_z \times \frac{\partial \vec{\mathcal{E}}_t}{\partial z} \right] = -\frac{\partial \vec{\mathcal{E}}_t}{\partial z} \quad (1.11a)$$

$$\vec{a}_z \times \left[ \vec{a}_z \times \frac{\partial \vec{\mathcal{H}}_t}{\partial z} \right] = -\frac{\partial \vec{\mathcal{H}}_t}{\partial z} \quad (1.11b)$$

as illustrated in Figure 1.4. Therefore, Eqs. (1.10) become

$$-\frac{\partial \vec{\mathcal{E}}_t}{\partial z} = -\mu \left[ \vec{a}_z \times \frac{\partial \vec{\mathcal{H}}_t}{\partial t} \right] \quad (1.12a)$$

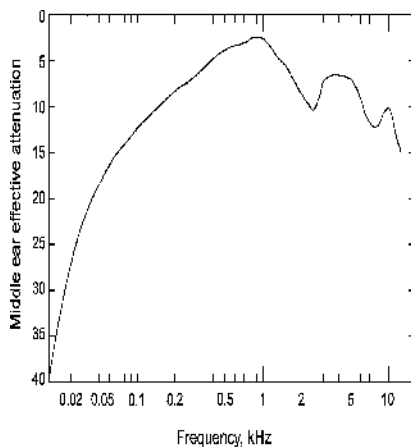


**FIGURE 1.4** Illustration of the identity  $\vec{a}_z \times (\vec{a}_z \times \vec{\mathcal{E}}_t) = -\vec{\mathcal{E}}_t$ .

$$-\frac{\partial \vec{\mathcal{H}}_t}{\partial z} = \sigma(\vec{a}_z \times \vec{\mathcal{E}}_t) + \varepsilon \left[ \vec{a}_z \times \frac{\partial \vec{\mathcal{E}}_t}{\partial t} \right] \quad (1.12b)$$

Taking the partial derivative of both sides of (1.12) with respect to  $z$ , taking the partial derivative of both sides of (1.4a) and (1.4b) with respect to  $t$ , and substituting gives the second-order *vector* partial differential equations that the transverse field vectors must satisfy:

$$\frac{\partial^2 \vec{\mathcal{E}}_t}{\partial z^2} = \mu\sigma \frac{\partial \vec{\mathcal{E}}_t}{\partial t} + \mu\varepsilon \frac{\partial^2 \vec{\mathcal{E}}_t}{\partial t^2} \quad (1.13a)$$

$$\frac{\partial^2 \vec{\mathcal{H}}_t}{\partial z^2} = \mu\sigma \frac{\partial \vec{\mathcal{H}}_t}{\partial t} + \mu\varepsilon \frac{\partial^2 \vec{\mathcal{H}}_t}{\partial t^2} \quad (1.13b)$$

Substituting (1.6) into (1.13) yields the second-order *scalar* partial differential equations in terms of the scalar functions  $e(z, t)$  and  $h(z, t)$  as

$$\frac{\partial^2 e(z, t)}{\partial z^2} = \mu\sigma \frac{\partial e(z, t)}{\partial t} + \mu\varepsilon \frac{\partial^2 e(z, t)}{\partial t^2} \quad (1.14a)$$

$$\frac{\partial^2 h(z, t)}{\partial z^2} = \mu\sigma \frac{\partial h(z, t)}{\partial t} + \mu\varepsilon \frac{\partial^2 h(z, t)}{\partial t^2} \quad (1.14b)$$

Once (1.14) are solved for the scalar functions  $e(z, t)$  and  $h(z, t)$ , we can determine the transverse field vectors by solving for the scalar potential functions in the transverse plane,  $\nabla_t \phi(x, y)$  and  $\nabla_t \psi(x, y)$ , and taking the products as in (1.6). This second problem, solving for the scalar potential functions in the transverse plane, depends only on the cross-sectional dimensions of the transmission line.

Now let us consider the case where the medium is *lossless*, that is,  $\sigma = 0$ . In this case, Eqs. (1.14) reduce to

$$\frac{\partial^2 e(z, t)}{\partial z^2} = \mu\varepsilon \frac{\partial^2 e(z, t)}{\partial t^2} \quad (1.15a)$$

$$\frac{\partial^2 h(z, t)}{\partial z^2} = \mu\varepsilon \frac{\partial^2 h(z, t)}{\partial t^2} \quad (1.15b)$$

The general solutions of these consist of waves traveling in the  $+z$  and  $-z$  directions as in [A.1]

$$e(z, t) = e^+ \left( t - \frac{z}{v} \right) + e^- \left( t + \frac{z}{v} \right) \quad (1.16a)$$

$$h(z, t) = h^+ \left( t - \frac{z}{v} \right) + h^- \left( t + \frac{z}{v} \right) \quad (1.16b)$$

where the velocity of propagation is

$$v = \frac{1}{\sqrt{\mu\varepsilon}} \quad (1.17)$$

Observe that in these solutions, the variables  $z$  and  $t$  can only appear together as  $t \pm (z/v)$ . The function  $e^+(t - (z/v))$  represents a *forward-traveling wave* since as  $t$  progresses,  $z$  must increase to keep the argument constant and track corresponding points on the waveform. Similarly, the function  $e^-(t + (z/v))$  represents a *backward-traveling wave* traveling in the  $-z$  direction. The solutions for the electric and magnetic field vectors may be obtained by substituting (1.16a) and (1.16b) into (1.6) to yield

$$\vec{\mathcal{E}}_t(x, y, z, t) = \underbrace{e^+ \left( t - \frac{z}{v} \right) \nabla_t \phi(x, y)}_{\vec{\mathcal{E}}_t^+} + \underbrace{e^- \left( t + \frac{z}{v} \right) \nabla_t \phi(x, y)}_{\vec{\mathcal{E}}_t^-} \quad (1.18a)$$

$$\begin{aligned} \vec{\mathcal{H}}_t(x, y, z, t) &= \underbrace{h^+ \left( t - \frac{z}{v} \right) \nabla_t \psi(x, y)}_{\vec{\mathcal{H}}_t^+} + \underbrace{h^- \left( t + \frac{z}{v} \right) \nabla_t \psi(x, y)}_{\vec{\mathcal{H}}_t^-} \\ &= \frac{1}{\eta} e^+ \left( t - \frac{z}{v} \right) [\vec{a}_z \times \nabla_t \phi(x, y)] - \frac{1}{\eta} e^- \left( t + \frac{z}{v} \right) [\vec{a}_z \times \nabla_t \phi(x, y)] \end{aligned} \quad (1.18b)$$

where the *intrinsic impedance* of the medium is

$$\eta = \sqrt{\frac{\mu}{\varepsilon}} \quad (1.19)$$

These may be proven by direct substitution into (1.12) and recalling that  $\vec{a}_z \times [\vec{a}_z \times \nabla_t \phi] = -\nabla_t \phi$  and  $\vec{a}_z \times [\vec{a}_z \times \nabla_t \psi] = -\nabla_t \psi$ . Hence we may write the transverse fields as

$$\vec{\mathcal{E}}_t(x, y, z, t) = \vec{\mathcal{E}}_t^+(x, y, z, t) + \vec{\mathcal{E}}_t^-(x, y, z, t) \quad (1.20a)$$

$$\begin{aligned} \vec{\mathcal{H}}_t(x, y, z, t) &= \vec{\mathcal{H}}_t^+(x, y, z, t) + \vec{\mathcal{H}}_t^-(x, y, z, t) \\ &= \frac{1}{\eta} \vec{a}_z \times \vec{\mathcal{E}}_t^+(x, y, z, t) - \frac{1}{\eta} \vec{a}_z \times \vec{\mathcal{E}}_t^-(x, y, z, t) \end{aligned} \quad (1.20b)$$

Consequently, we may indicate the vector relation between the forward- and backward-traveling electric and magnetic field components as

$$\vec{\mathcal{H}}_t^\pm = \pm \frac{1}{\eta} \vec{a}_z \times \vec{\mathcal{E}}_t^\pm \quad (1.21)$$

with the sign depending on whether we are considering the backward- or forward-traveling wave component.

If the time variation of the field vectors is sinusoidal, we use phasor notation [A.2,A.5]:

$$\vec{\mathcal{E}}_t(x, y, z, t) = \text{Re}\left\{\vec{E}_t(x, y, z)e^{j\omega t}\right\} \quad (1.22a)$$

$$\vec{\mathcal{H}}_t(x, y, z, t) = \text{Re}\left\{\vec{H}_t(x, y, z)e^{j\omega t}\right\} \quad (1.22b)$$

where the phasor transverse field vectors are complex valued and denoted as  $\vec{E}_t$  and  $\vec{H}_t$ . We will denote complex-valued quantities with a caret ( $\hat{\cdot}$ ) over the quantity. In terms of the scalar functions  $e(z, t)$  and  $h(z, t)$ , these become

$$e(z, t) = \text{Re}\{\hat{e}(z)e^{j\omega t}\} \quad (1.23a)$$

$$h(z, t) = \text{Re}\{\hat{h}(z)e^{j\omega t}\} \quad (1.23b)$$

Replacing time derivatives with  $\frac{\partial}{\partial t} = j\omega$  in (1.15) gives the *phasor form* of the differential equations for a lossless medium,  $\sigma = 0$ , as

$$\frac{d^2\hat{e}(z)}{dz^2} = -\omega^2\mu\varepsilon\hat{e}(z) \quad (1.24a)$$

$$\frac{d^2\hat{h}(z)}{dz^2} = -\omega^2\mu\varepsilon\hat{h}(z) \quad (1.24b)$$

The solutions to these equations are [A.1]

$$\hat{e}(z) = \hat{e}^+e^{-j\beta z} + \hat{e}^-e^{j\beta z} \quad (1.25a)$$

$$\hat{h}(z) = \hat{h}^+e^{-j\beta z} + \hat{h}^-e^{j\beta z} \quad (1.25b)$$

where the complex undetermined constants are denoted as  $\hat{e}^\pm$  and  $\hat{h}^\pm$ , and the phase constant is denoted as

$$\beta = \omega\sqrt{\mu\varepsilon} \quad (\text{rad/m}) \quad (1.26)$$

The terms  $e^{\pm j\beta z} = 1\angle(\pm\beta z)$  represent a phase shift as the single-frequency, sinusoidal waves propagate in the  $z$  direction. Substituting (1.25) into (1.6) gives the phasor field

vectors:

$$\vec{\hat{E}}_t(x, y, z) = \underbrace{\hat{e}^+ \nabla_t \phi(x, y)}_{\vec{\hat{E}}^+(x, y)} e^{-j\beta z} + \underbrace{\hat{e}^- \nabla_t \phi(x, y)}_{\vec{\hat{E}}^-(x, y)} e^{j\beta z} \quad (1.27a)$$

$$\begin{aligned} \vec{\hat{H}}_t(x, y, z) &= \underbrace{\hat{h}^+ \nabla_t \psi(x, y)}_{\vec{\hat{H}}^+(x, y)} e^{-j\beta z} + \underbrace{\hat{h}^- \nabla_t \psi(x, y)}_{\vec{\hat{H}}^-(x, y)} e^{j\beta z} \\ &= \frac{1}{\eta} \hat{e}^+ \vec{a}_z \times \nabla_t \phi(x, y) e^{-j\beta z} - \frac{1}{\eta} \hat{e}^- \vec{a}_z \times \nabla_t \phi(x, y) e^{j\beta z} \end{aligned} \quad (1.27b)$$

and once again

$$\vec{\hat{H}}^\pm = \pm \frac{1}{\eta} \vec{a}_z \times \vec{\hat{E}}^\pm \quad (1.28)$$

The time-domain expressions are obtained by multiplying (1.27) by  $e^{j\omega t}$  and taking the real part of the result according to (1.22) [A.1]. For example, the  $x$  component of the transverse electric field vector and the  $y$  component of the magnetic field vector are

$$\mathcal{E}_x(x, y, z, t) = E_{mx}^+ \cos(\omega t - \beta z + \theta_x^+) + E_{mx}^- \cos(\omega t + \beta z + \theta_x^-) \quad (1.29a)$$

$$\mathcal{H}_y(x, y, z, t) = \frac{1}{\eta} E_{mx}^+ \cos(\omega t - \beta z + \theta_x^+) - \frac{1}{\eta} E_{mx}^- \cos(\omega t + \beta z + \theta_x^-) \quad (1.29b)$$

where the  $x$  components of the undetermined complex field components are functions of  $x$  and  $y$  and are denoted as  $\hat{E}_x^\pm(x, y) = E_{mx}^\pm \angle \theta_x^\pm$ . The phase velocity of the waves is obtained by setting the argument of each cosine in (1.29) to a constant (in order to follow a point on the waveform) and differentiating to yield  $\omega dt - \beta dz = 0$  or  $v = (dz/dt) = (\omega/\beta)$ . Substituting (1.26) gives the wave constant phase velocity as

$$\begin{aligned} v &= \frac{\omega}{\beta} \\ &= \frac{1}{\sqrt{\mu\epsilon}} \end{aligned} \quad (1.30)$$

The phase constant  $\beta$  has the unit of rad/m and represents a phase shift as the wave propagates through the medium. A *wavelength*, denoted as  $\lambda$ , is the distance (in meters) a single-frequency, sinusoidal wave must travel to change phase by  $2\pi$  radians or  $360^\circ$ . Hence,  $\beta\lambda = 2\pi$  and therefore

$$\lambda = \frac{2\pi}{\beta} = \frac{v}{f} \quad (1.31)$$

If we now consider adding conductive losses to the medium,  $\sigma \neq 0$ , this adds a transverse conductive current term,  $\vec{J}_t = \sigma \vec{\mathcal{E}}_t$ , to Ampere's law given in Eq. (1.1b). Replacing time derivatives with  $j\omega$  in the second-order differential equations in (1.14) gives the corresponding phasor differential equations for the case of a lossy medium as

$$\begin{aligned} \frac{d^2 \hat{e}(z)}{dz^2} &= j\omega\mu\sigma \hat{e}(z) + (j\omega)^2(\mu\varepsilon) \hat{e}(z) \\ &= j\omega\mu(\sigma + j\omega\varepsilon) \hat{e}(z) \\ &= \hat{\gamma}^2 \hat{e}(z) \end{aligned} \quad (1.32a)$$

$$\begin{aligned} \frac{d^2 \hat{h}(z)}{dz^2} &= j\omega\mu\sigma \hat{h}(z) + (j\omega)^2(\mu\varepsilon) \hat{h}(z) \\ &= j\omega\mu(\sigma + j\omega\varepsilon) \hat{h}(z) \\ &= \hat{\gamma}^2 \hat{h}(z) \end{aligned} \quad (1.32b)$$

where the *propagation constant* is

$$\begin{aligned} \hat{\gamma} &= \sqrt{j\omega\mu(\sigma + j\omega\varepsilon)} \\ &= \alpha + j\beta \end{aligned} \quad (1.33)$$

The solutions to these equations are [A.1]

$$\hat{e}(z) = \hat{e}^+ e^{-\alpha z} e^{-j\beta z} + \hat{e}^- e^{\alpha z} e^{j\beta z} \quad (1.34a)$$

$$\hat{h}(z) = \hat{h}^+ e^{-\alpha z} e^{-j\beta z} + \hat{h}^- e^{\alpha z} e^{j\beta z} \quad (1.34b)$$

Hence, the phase constant is the imaginary part of the propagation constant and is no longer  $\omega\sqrt{\mu\varepsilon}$ , as was the case for a lossless medium, that is,  $\beta \neq \omega\sqrt{\mu\varepsilon}$ . In addition, the real part of the propagation constant,  $\alpha$ , is said to be the *attenuation constant* and it represents losses in the medium as we will see later. The phasor solutions for the phasor field vectors for this case of a lossy medium,  $\sigma \neq 0$ , are

$$\vec{\hat{E}}_t(x, y, z) = \underbrace{\hat{e}^+ \nabla_t \phi(x, y)}_{\vec{\hat{E}}^+(x, y)} e^{-\alpha z} e^{-j\beta z} + \underbrace{\hat{e}^- \nabla_t \phi(x, y)}_{\vec{\hat{E}}^-(x, y)} e^{\alpha z} e^{j\beta z} \quad (1.35a)$$

$$\begin{aligned} \vec{\hat{H}}_t(x, y, z) &= \underbrace{\hat{h}^+ \nabla_t \psi(x, y)}_{\vec{\hat{H}}^+(x, y)} e^{-\alpha z} e^{-j\beta z} + \underbrace{\hat{h}^- \nabla_t \psi(x, y)}_{\vec{\hat{H}}^-(x, y)} e^{\alpha z} e^{j\beta z} \\ &= \frac{1}{\hat{\eta}} \hat{e}^+ \vec{a}_z \times \nabla_t \phi(x, y) e^{-\alpha z} e^{-j\beta z} - \frac{1}{\hat{\eta}} \hat{e}^- \vec{a}_z \times \nabla_t \phi(x, y) e^{\alpha z} e^{j\beta z} \end{aligned} \quad (1.35b)$$

where the intrinsic impedance now becomes complex as

$$\begin{aligned}\hat{\eta} &= \sqrt{\frac{j\omega\mu}{\sigma + j\omega\varepsilon}} \\ &= \eta \angle \theta_\eta \\ &= \eta e^{j\theta_\eta}\end{aligned}\tag{1.36}$$

and once again

$$\vec{H}^\pm = \pm \frac{1}{\hat{\eta}} \vec{a}_z \times \vec{E}^\pm\tag{1.37}$$

Again, the time-domain expressions are obtained by multiplying (1.35a) and (1.35b) by  $e^{j\omega t}$  and taking the real part of the result according to (1.22) [A.1]. For example, the  $x$  component of the transverse electric field vector and the  $y$  component of the magnetic field vector are

$$\mathcal{E}_x(x, y, z, t) = E_{mx}^+ e^{-\alpha z} \cos(\omega t - \beta z + \theta_x^+) + E_{mx}^- e^{\alpha z} \cos(\omega t + \beta z + \theta_x^-)\tag{1.38a}$$

$$\begin{aligned}\mathcal{H}_y(x, y, z, t) &= \frac{1}{\eta} E_{mx}^+ e^{-\alpha z} \cos(\omega t - \beta z + \theta_x^+ - \theta_\eta) \\ &\quad - \frac{1}{\eta} E_{mx}^- e^{\alpha z} \cos(\omega t + \beta z + \theta_x^- - \theta_\eta)\end{aligned}\tag{1.38b}$$

Thus, in addition to a phase shift represented by  $e^{\pm j\beta z}$ , the waves suffer an *attenuation* of their amplitudes as represented by  $e^{\pm \alpha z}$ . We will find these properties of the TEM mode of propagation arising in various guises throughout our examination of MTLs.

### 1.3 THE TRANSMISSION-LINE EQUATIONS: A PREVIEW

Consider a two-conductor transmission line that has two conductors of uniform cross section that are parallel to each other and the  $z$  axis as shown in Figure 1.5(a). The conductors are considered to be perfect conductors (lossless,  $\sigma = \infty$ ), and the surrounding medium is homogeneous and lossy with parameters  $\mu = \mu_0$ ,  $\varepsilon = \varepsilon_r \varepsilon_0$ ,  $\sigma$ . The transverse electric and magnetic fields are shown in Figure 1.5(b) in the transverse  $x$ - $y$  plane. In order to satisfy the boundary conditions on the surfaces of the perfect conductors, the electric fields must be normal to the conductor surfaces and the magnetic fields must be tangent to the conductor surfaces [A.1]. It should be noted that because these conductors are assumed to be perfect conductors, the boundary conditions also show that the magnetic field intensity vector  $\vec{\mathcal{H}}$  must be tangent to the surfaces of these perfect conductors and induces a surface current to flow on these conductors [A.1]. Since the magnetic field lies in the transverse plane, these induced

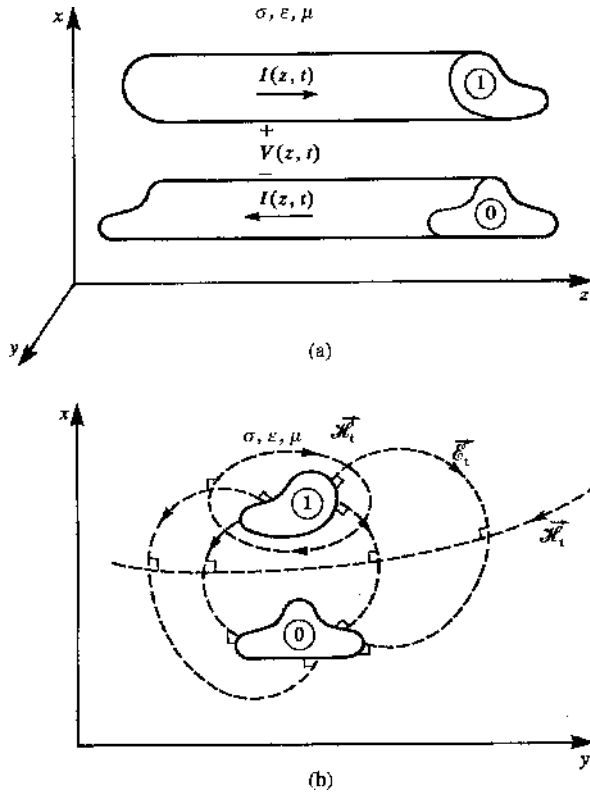


**FIGURE 1.5** Illustration of (a) the current and voltage and (b) the TEM fields for a two-conductor line.

currents on the surfaces of the conductors are directed in the  $z$  direction [A.1]. These are the transmission-line currents. In addition, since the conductors are assumed to be perfect conductors, these boundary conditions show that the electric flux density vector  $\vec{D} = \epsilon\vec{E}$  that is normal to the surfaces of the conductors induces a surface charge density on these conductors from which the transverse electric field vectors emanate [A.1]. In addition, the transverse electric and magnetic field lines are everywhere in this transverse plane orthogonal to each other.

### 1.3.1 Unique Definition of Voltage and Current for the TEM Mode of Propagation

In the previous section, it was shown that the electric and magnetic field vectors in the transverse ( $x-y$ ) plane satisfy a static distribution. In other words, the electric and magnetic fields in the transverse plane have distributions identical to dc fields even though they vary with time. Hence we may uniquely define a voltage between the two conductors by integrating the component of the electric field tangent to a contour  $c$  in the

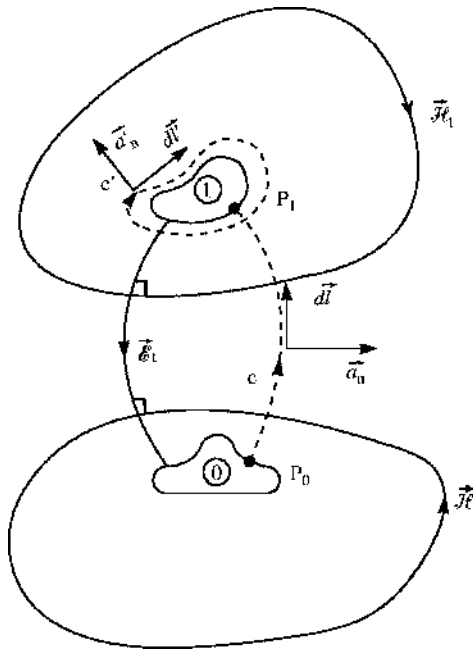


**FIGURE 1.6** Illustrations of the contours and surfaces for the definitions of voltage and current for a two-conductor line.

transverse plane between two points on each conductor as shown in Figure 1.6 [A.1]:

$$\begin{aligned}
 V(z, t) &= - \int_c \vec{E}_t \cdot d\vec{l} \\
 &= - \int_{P_0}^{P_1} \vec{E}_t \cdot d\vec{l}
 \end{aligned}
 \tag{1.39}$$

This may be directly shown by substituting the relation between the transverse electric field and the scalar potential function in (1.6a):

$$\begin{aligned}
 V(z, t) &= - \int_{P_0}^{P_1} e(z, t) \nabla_t \phi(x, y) \cdot d\vec{l} \\
 &= -e(z, t) \int_{P_0}^{P_1} \nabla_t \phi(x, y) \cdot d\vec{l} \\
 &= -e(z, t) [\phi_1 - \phi_0]
 \end{aligned}
 \tag{1.40}$$

where  $\phi_0$  and  $\phi_1$  are the potentials on the surfaces of the two conductors in this transverse plane [A.1]. Because the conductors are assumed to be perfect conductors,

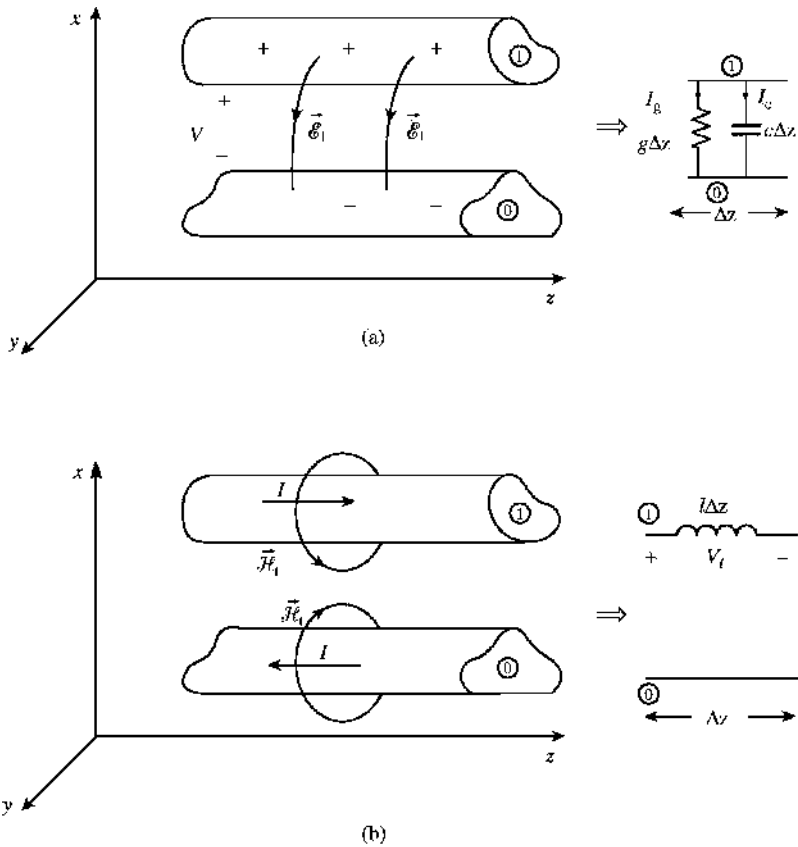


FIGURE 1.7 Illustrations of the intuitive meaning of the per-unit-length parameters.

the potentials are the same at all points on their surfaces, and because this transverse electric field is conservative, this integral is independent of path in the transverse plane and is therefore unique. Similarly, we can uniquely define current as the line integral of the transverse magnetic field around a closed path  $c'$  encircling the top conductor as shown in Figure 1.6 [A.1]:

$$I(z, t) = \oint_{c'} \vec{\mathcal{H}}_t \cdot d\vec{l}' \tag{1.41}$$

Since there is no component of the electric field in the  $z$  direction, there is no displacement current in the  $z$  direction and this reduces to Ampere's law for static conditions [A.1]. Hence, this result is independent of path taken around this conductor so long as it encircles only this conductor.

### 1.3.2 Defining the Per-Unit-Length Parameters

Figure 1.7 gives an intuitive view of the essential ingredients of the transmission-line equations: the per-unit-length parameters of the line. Figure 1.7(a) shows the effect of the transverse electric field  $\vec{\mathcal{E}}_t$  that is directed from the top conductor to the bottom conductor. The transverse electric field lines begin on positive charge on the surface of the upper conductor and terminate on negative charge on the surface of the lower conductor. This transverse electric field will cause two currents in the surrounding dielectric in this transverse plane that are directed from the top conductor to the lower conductor:

$$\underbrace{I_t(z, t)}_{\text{transverse current}} = \underbrace{I_g(z, t)}_{\text{conduction current}} + \underbrace{I_c(z, t)}_{\text{displacement current}} \quad (1.42)$$

A transverse conduction current  $\vec{J}_t = \sigma \vec{\mathcal{E}}_t$ , is induced by this transverse electric field to flow in the lossy medium due to its conductivity  $\sigma$  from the top conductor to the bottom conductor in this transverse plane. This effect is represented for a section of line of length  $\Delta z$  by a conductance. For a uniform line, this effect is uniformly distributed along the line. Hence if a section of line of length  $\Delta z$  has a total conductance  $G$ , then a *per-unit-length conductance*  $g$  whose units are S/m, is given by

$$g = \underbrace{\lim}_{\Delta z \rightarrow 0} \frac{G}{\Delta z} \quad (\text{S/m}) \quad (1.43)$$

The transverse current flowing from the top conductor to the bottom conductor is related to the voltage between the two conductors by

$$I_g(z, t) = g \Delta z V(z, t) \quad (1.44)$$

In addition, since charge is stored on the top and bottom conductors, we essentially have a capacitance between the two conductors. If a section of line of length  $\Delta z$  has a total capacitance  $C$ , the charge is related to the voltage by  $Q = CV$ . For a uniform line, this effect is uniformly distributed along the line. Hence if a section of line of length  $\Delta z$  has a total capacitance  $C$ , then the *per-unit-length capacitance*  $c$  whose units are F/m, is given by

$$c = \underbrace{\lim}_{\Delta z \rightarrow 0} \frac{C}{\Delta z} \quad (\text{F/m}) \quad (1.45)$$

The (displacement) current flowing in the transverse plane from the top conductor to the bottom conductor is

$$I_c(z, t) = c \Delta z \frac{\partial V(z, t)}{\partial t} \quad (1.46)$$

Consider Figure 1.7(b). The current flowing along the top conductor and returning along the bottom conductor will generate a magnetic field intensity in the transverse plane,  $\vec{\mathcal{H}}_t$ . The transverse magnetic flux density is [A.1]  $\vec{\mathcal{B}}_t = \mu \vec{\mathcal{H}}_t$  Wb/m<sup>2</sup>. This produces a magnetic flux  $\psi = \int_S \vec{\mathcal{B}}_t \cdot d\vec{s}$  through the surface that lies between the two conductors. A section of line will therefore have a total inductance  $L$ . For a uniform line, this effect is uniformly distributed along the line. Hence if a section of line of length  $\Delta z$  has a total inductance  $L$ , then a *per-unit-length inductance*  $l$  whose units are H/m, is given by

$$l = \lim_{\Delta z \rightarrow 0} \frac{L}{\Delta z} \quad (\text{H/m}) \quad (1.47)$$

This will produce a longitudinal voltage drop around the loop contained by the two conductors of

$$V_l(z, t) = l \Delta z \frac{\partial I(z, t)}{\partial t} \quad (1.48)$$

Note that this inductance is a property of the loop formed by the two conductors and as such may be placed in either the top or the bottom conductor. It cannot be uniquely assigned to either conductor.

Adjacent to each of these figures is a lumped-circuit model of an electrically small  $\Delta z$  section. Figure 1.8(a) combines these into one model. The total line length is represented as a continuum of these, as shown in Figure 1.8(b). From the per-unit-length model of the line in Figure 1.8(a), we can obtain the transmission-line equations by using Kirchhoff's voltage (KVL) and current (KCL) laws [A.2,A.5]. Writing KVL at the left and right ends of this circuit gives

$$V(z + \Delta z, t) - V(z, t) = -l \Delta z \frac{\partial I(z, t)}{\partial t} \quad (1.49a)$$

and writing KCL at the top right node gives

$$I(z + \Delta z) - I(z, t) = -g \Delta z V(z + \Delta z, t) - c \Delta z \frac{\partial V(z + \Delta z, t)}{\partial t} \quad (1.49b)$$

Dividing (1.49) by  $\Delta z$  and taking the limit as  $\Delta z \rightarrow 0$  yields the *transmission-line equations*:

$$\frac{\partial V(z, t)}{\partial z} = -l \frac{\partial I(z, t)}{\partial t} \quad (1.50a)$$

$$\frac{\partial I(z, t)}{\partial z} = -g V(z, t) - c \frac{\partial V(z, t)}{\partial t} \quad (1.50b)$$

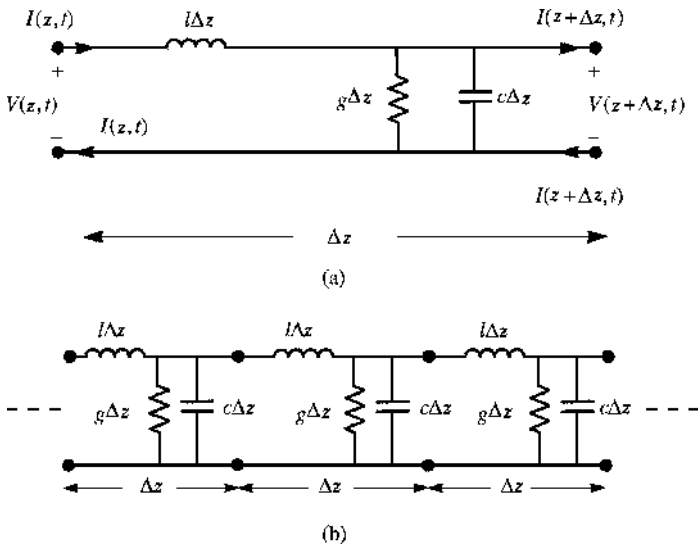


FIGURE 1.8 The per-unit-length equivalent circuit for a two-conductor line.

The above is an intuitive view of the per-unit-length line parameters. In order to compute values of these parameters, we need more precise definitions of them. First, we compute the per-unit-length inductance. We desire to compute the total magnetic flux through a surface between the two conductors that is of differential length along the line of  $\Delta z$ , and the surface is uniform along the line, that is, does not vary with  $z$ . The desired surface is shown in Figure 1.9(a) where the unit normal to the surface  $s$  is denoted as  $\vec{a}_n$ . A cross section in the transverse plane is shown in Figure 1.6. The magnetic flux density vector is  $\vec{\mathcal{B}}_t = \mu \vec{\mathcal{H}}_t$  and the total magnetic flux through the surface is the surface integral of this over the surface:

$$\psi = \int_s \mu \vec{\mathcal{H}}_t \cdot \vec{a}_n ds \tag{1.51}$$

The total inductance is the ratio of the magnetic flux through this surface to the current that caused it:

$$l\Delta z = - \frac{\int_s \mu \vec{\mathcal{H}}_t \cdot \vec{a}_n ds}{I(z, t)} \tag{1.52}$$

where  $l$  is the per-unit-length inductance desired. We have defined the closed contour around the perimeter of this surface as  $c$ . The differential path length along this contour is denoted by  $d\vec{l}$ , and the normal to the surface is denoted as  $\vec{a}_n$ , as shown in Figure 1.6. The definition of the direction of the desired flux through this surface is according to the right-hand rule with respect to the current. Placing the thumb in the

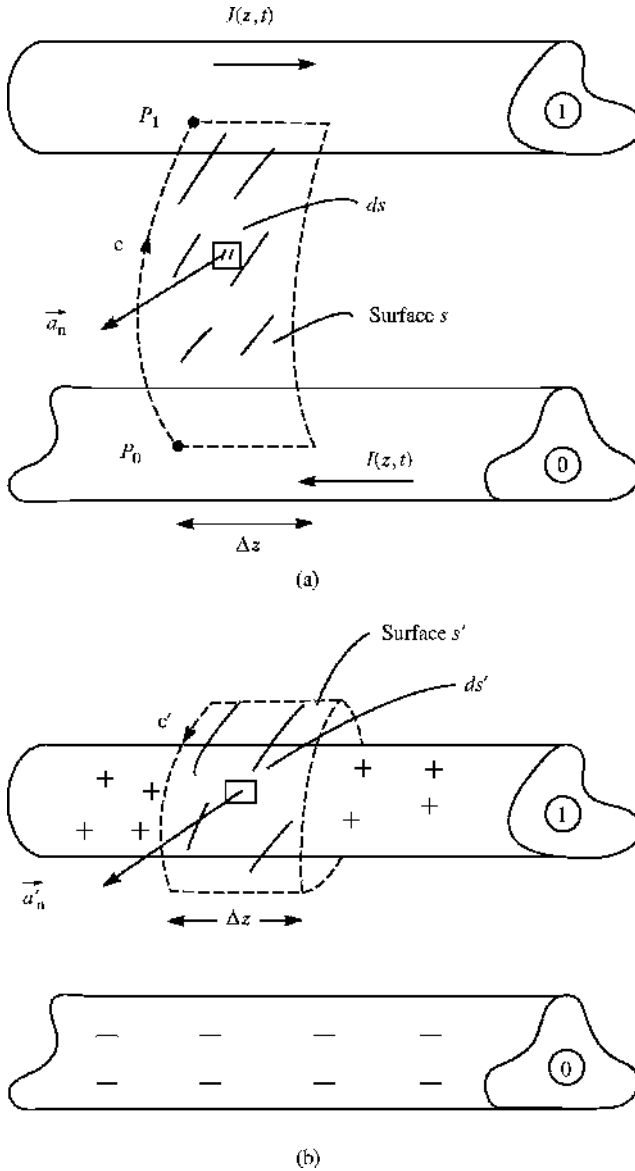


**FIGURE 1.9** Contours and surfaces for the derivation of the transmission-line equations: (a) derivation of the voltage change equation, and (b) derivation of the current change equation.

direction of the current (into the page in the  $+z$  direction for the top conductor and out of the page in the  $-z$  direction for the bottom conductor) gives the direction of the desired flux as clockwise when looking in the  $+z$  direction, as in Figure 1.6, which is opposite to the direction of the normal to the surface,  $\vec{a}_n$ . Hence, a minus sign is required in (1.52). For a length of the surface of  $\Delta z$  that is considered differentially

small, the flux through the surface does not vary with  $z$ . Hence we may remove this dimension from the integral in (1.52). Therefore, as we shrink the length of the surface to zero, the desired flux is obtained by simply integrating along the contour  $c$  to give

$$l\Delta z = -\frac{\Delta z\mu \int_c \vec{\mathcal{H}}_t \cdot \vec{a}_n dl}{I(z, t)} \quad (1.53a)$$

or

$$l = -\frac{\mu \int_c \vec{\mathcal{H}}_t \cdot \vec{a}_n dl}{I(z, t)} \quad (1.53b)$$

Substituting the definition of current given in (1.41) gives

$$l = -\mu \frac{\int_c \vec{\mathcal{H}}_t \cdot \vec{a}_n dl}{\oint_{c'} \vec{\mathcal{H}}_t \cdot d\vec{l}'} \quad (1.54)$$

Next, consider obtaining the per-unit-length capacitance  $c$  as illustrated in Figure 1.9(b). Charge of equal magnitude but opposite sign is distributed along each conductor and around their peripheries. We desire to compute the total charge contained on the top conductor along a differential length along the line of  $\Delta z$ . The electric flux density vector on the surface of the perfect conductor is  $\vec{\mathcal{D}}_t = \varepsilon \vec{\mathcal{E}}_t$  and, according to the boundary conditions on the surface of this perfect conductor, is normal to the surface [A.1]. In order to determine the charge on the conductor surface, we surround it with a closed surface  $s'$  that is just off the surface of the conductor and determine the total electric flux through that surface. A cross section in the transverse plane is shown in Figure 1.6, where the unit normal to the surface  $s'$  is  $\vec{a}'_n$ . The total capacitance is the ratio of this total charge to the voltage between the two conductors:

$$c\Delta z = \frac{\varepsilon \oint_{s'} \vec{\mathcal{E}}_t \cdot \vec{a}'_n ds'}{V(z, t)} \quad (1.55)$$

where  $s'$  is the closed surface and  $c$  is the per-unit-length capacitance desired. We have defined the closed contour around the perimeter of this surface as  $c'$ . The differential path length along this contour is denoted by  $d\vec{l}'$  and the normal to the surface is denoted as  $\vec{a}'_n$ . Note that these surfaces and contours are designated with primes to distinguish them from the surfaces and contours used to determine the inductance above. Since the transverse electric field and electric flux density vector is from the upper conductor to the lower conductor, it is directed out of this closed surface  $s'$  giving the enclosed

charge as positive. For a length of the surface of  $\Delta z$  that is considered differentially small, the flux through the surface does not vary with  $z$ . Hence we may remove this dimension from the integral in (1.55). Therefore, as we shrink the length of the surface to zero, the desired flux is obtained by simply integrating along the closed contour  $c'$  to give

$$c\Delta z = \frac{\Delta z \varepsilon \oint_{c'} \vec{\mathcal{E}}_t \cdot \vec{a}'_n dl'}{V(z, t)} \quad (1.56a)$$

or

$$c = \frac{\varepsilon \oint_{c'} \vec{\mathcal{E}}_t \cdot \vec{a}'_n dl'}{V(z, t)} \quad (1.56b)$$

Substituting the definition of voltage given in (1.39) gives

$$c = \varepsilon \frac{\oint_{c'} \vec{\mathcal{E}}_t \cdot \vec{a}'_n dl'}{- \int_c \vec{\mathcal{E}}_t \cdot d\vec{l}} \quad (1.57)$$

In order to determine the per-unit-length conductance  $g$ , we need to determine the transverse conduction current. The transverse conduction current is obtained by integrating  $\sigma \vec{\mathcal{E}}_t$  over the closed surface  $s'$  as

$$g\Delta z = \frac{\sigma \oint_{s'} \vec{\mathcal{E}}_t \cdot \vec{a}'_n ds'}{V(z, t)} \quad (1.58)$$

Once again, we assume that the length of the surface along the line  $\Delta z$  is differentially small so that this dimension may be removed from the integral in (1.58), and the desired transverse current is obtained by simply integrating along the contour  $c'$  to give

$$g\Delta z = \frac{\Delta z \sigma \oint_{c'} \vec{\mathcal{E}}_t \cdot \vec{a}'_n dl'}{V(z, t)} \quad (1.59a)$$

or

$$g = \frac{\sigma \oint_{c'} \vec{\mathcal{E}}_t \cdot \vec{a}'_n dl'}{V(z, t)} \quad (1.59b)$$

Substituting the definition of voltage given in (1.39) gives

$$g = \sigma \frac{\oint \vec{\mathcal{E}}_t \cdot \vec{a}'_n dl'}{-\int_c \vec{\mathcal{E}}_t \cdot d\vec{l}} \quad (1.60)$$

In Section 1.3.4, we will show that the per-unit-length parameters satisfy the following relations:

$$lc = \mu\varepsilon \quad (1.61)$$

$$gl = \sigma\mu \quad (1.62)$$

Taking the ratio of (1.61) and (1.62) or the ratio of (1.60) and (1.57) gives another relation:

$$\frac{g}{c} = \frac{\sigma}{\varepsilon} \quad (1.63)$$

Hence for a *homogeneous* medium surrounding the conductors that is characterized by the parameters  $\sigma$ ,  $\varepsilon$ , and  $\mu$ , we only need to determine one of the three parameters. For example, if we determine the per-unit-length capacitance  $c$ , then the other two parameters are obtained in terms of  $c$  as  $l = (\mu\varepsilon/c)$  and  $g = (\sigma/\varepsilon)c$ .

### 1.3.3 Obtaining the Transmission-Line Equations from the Transverse Electromagnetic Field Equations

In Section 1.2 we showed that, for the TEM mode, the transverse field vectors satisfy the relations in (1.12):

$$-\frac{\partial \vec{\mathcal{E}}_t}{\partial z} = -\mu \left[ \vec{a}_z \times \frac{\partial \vec{\mathcal{H}}_t}{\partial t} \right] \quad (1.12a)$$

$$-\frac{\partial \vec{\mathcal{H}}_t}{\partial z} = \sigma(\vec{a}_z \times \vec{\mathcal{E}}_t) + \varepsilon \left[ \vec{a}_z \times \frac{\partial \vec{\mathcal{E}}_t}{\partial t} \right] \quad (1.12b)$$

Integrating (1.12a) along contour  $c$  to define the line voltage as given in (1.39) gives

$$\frac{\partial V(z, t)}{\partial z} = -\mu \frac{\partial}{\partial t} \int_c (\vec{a}_z \times \vec{\mathcal{H}}_t) \cdot d\vec{l} \quad (1.64)$$

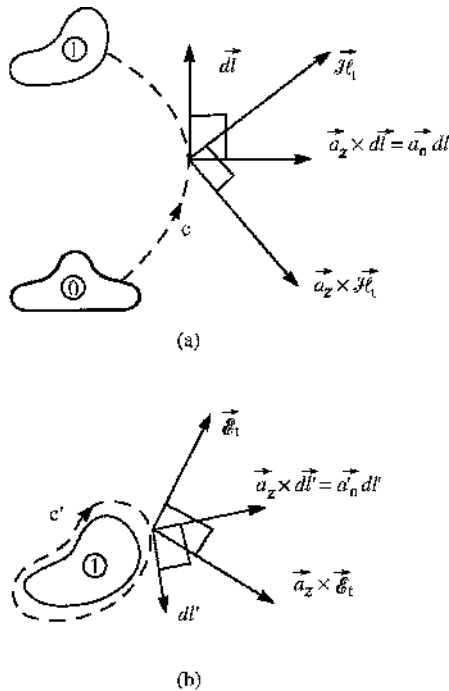


**FIGURE 1.10** Illustration of the derivation of certain vector identities.

From Figure 1.10(a), we observe the identities:

$$\begin{aligned}
 (\vec{a}_z \times \vec{\mathcal{H}}_t) \cdot d\vec{l} &= -\vec{\mathcal{H}}_t \cdot (\vec{a}_z \times d\vec{l}) \\
 &= -\vec{\mathcal{H}}_t \cdot \vec{a}_n dl
 \end{aligned}
 \tag{1.65}$$

Substituting this into (1.64), we obtain

$$\frac{\partial V(z, t)}{\partial z} = \mu \frac{\partial}{\partial t} \int_c \vec{\mathcal{H}}_t \cdot \vec{a}_n dl
 \tag{1.66}$$

From the definition of the per-unit-length inductance in (1.53b), this becomes the first transmission-line equation:

$$\frac{\partial V(z, t)}{\partial z} = -l \frac{\partial I(z, t)}{\partial t}
 \tag{1.67}$$

Similarly, integrating (1.12b) around the closed contour  $c'$  to define the line currents as in (1.41) gives

$$\frac{\partial I(z, t)}{\partial z} = -\sigma \oint_{c'} (\vec{a}_z \times \vec{\mathcal{E}}_t) \cdot d\vec{l}' - \varepsilon \frac{\partial}{\partial t} \oint_{c'} (\vec{a}_z \times \vec{\mathcal{E}}_t) \cdot d\vec{l}' \quad (1.68)$$

From Figure 1.10(b), we observe the identities

$$\begin{aligned} (\vec{a}_z \times \vec{\mathcal{E}}_t) \cdot d\vec{l}' &= -\vec{\mathcal{E}}_t \cdot (\vec{a}_z \times d\vec{l}') \\ &= \vec{\mathcal{E}}_t \cdot \vec{a}'_n dl' \end{aligned} \quad (1.69)$$

Substituting this into (1.68) yields

$$\frac{\partial I(z, t)}{\partial z} = -\sigma \oint_{c'} \vec{\mathcal{E}}_t \cdot \vec{a}'_n dl' - \varepsilon \frac{\partial}{\partial t} \oint_{c'} \vec{\mathcal{E}}_t \cdot \vec{a}'_n dl' \quad (1.70)$$

Observing the definitions of the per-unit-length capacitance and conductance in (1.56b) and (1.59b), respectively, this gives the second transmission-line equation

$$\frac{\partial I(z, t)}{\partial z} = -gV(z, t) - c \frac{\partial V(z, t)}{\partial t} \quad (1.71)$$

### 1.3.4 Properties of the Per-Unit-Length Parameters

In this section, we will prove the important relations between the per-unit-length parameters given in (1.61) and (1.62):

$$lc = \mu\varepsilon \quad (1.61)$$

$$gl = \sigma\mu \quad (1.62)$$

which also give the relation

$$\frac{g}{c} = \frac{\sigma}{\varepsilon} \quad (1.63)$$

The first-order transmission-line differential equations in (1.67) and (1.71) are coupled in that  $V$  and  $I$  appear in each equation. They can be converted to uncoupled second-order equations by differentiating (1.67) with respect to  $z$ , differentiating (1.71) with respect to  $t$ , and then substituting and reversing the process to yield

$$\frac{\partial^2 V(z, t)}{\partial z^2} = gl \frac{\partial V(z, t)}{\partial t} + lc \frac{\partial^2 V(z, t)}{\partial t^2} \quad (1.72a)$$

$$\frac{\partial^2 I(z, t)}{\partial z^2} = gl \frac{\partial I(z, t)}{\partial t} + lc \frac{\partial^2 I(z, t)}{\partial t^2} \quad (1.72b)$$

The transverse field vectors were shown to satisfy the second-order differential equations given in (1.13):

$$\frac{\partial^2 \vec{\mathcal{E}}_t}{\partial z^2} = \mu\sigma \frac{\partial \vec{\mathcal{E}}_t}{\partial t} + \mu\varepsilon \frac{\partial^2 \vec{\mathcal{E}}_t}{\partial t^2} \quad (1.13a)$$

$$\frac{\partial^2 \vec{\mathcal{H}}_t}{\partial z^2} = \mu\sigma \frac{\partial \vec{\mathcal{H}}_t}{\partial t} + \mu\varepsilon \frac{\partial^2 \vec{\mathcal{H}}_t}{\partial t^2} \quad (1.13b)$$

Integrating these according to (1.39) and (1.41) in order to write them in terms of the line voltage and current gives

$$\frac{\partial^2 V(z, t)}{\partial z^2} = \mu\sigma \frac{\partial V(z, t)}{\partial t} + \mu\varepsilon \frac{\partial^2 V(z, t)}{\partial t^2} \quad (1.73a)$$

$$\frac{\partial^2 I(z, t)}{\partial z^2} = \mu\sigma \frac{\partial I(z, t)}{\partial t} + \mu\varepsilon \frac{\partial^2 I(z, t)}{\partial t^2} \quad (1.73b)$$

Comparing (1.73) to (1.72), we observe the important relations between the per-unit-length parameters:

$$gl = \mu\sigma \quad (1.74a)$$

$$lc = \mu\varepsilon \quad (1.74b)$$

Alternatively, we may obtain a direct proof of these relations between the per-unit-length parameters in the following manner. Write the product of the per-unit-length inductance and capacitance from their definitions in (1.54) and (1.57) as

$$lc = -\mu \frac{\int_c \vec{\mathcal{H}}_t \cdot \vec{a}_n dl \int_c \vec{\mathcal{E}}_t \cdot \vec{a}'_n dl'}{\int_c \vec{\mathcal{H}}_t \cdot d\vec{l}' - \int_c \vec{\mathcal{E}}_t \cdot d\vec{l}} \varepsilon \quad (1.75)$$

We showed in Section 1.2 that, for a lossless medium ( $\sigma = 0$ ), the forward- and backward-traveling components of the waves are related by the intrinsic impedance of the medium as

$$\vec{\mathcal{E}}_t^\pm = \mp \eta (\vec{a}_z \times \vec{\mathcal{H}}_t^\pm) \quad (1.76a)$$

Taking the cross product of  $\vec{a}_z$  with both sides and using  $\vec{a}_z \times (\vec{a}_z \times \vec{\mathcal{H}}_t) = -\vec{\mathcal{H}}_t$  yields

$$\vec{\mathcal{H}}_t^\pm = \pm \frac{1}{\eta} (\vec{a}_z \times \vec{\mathcal{E}}_t^\pm) \quad (1.76b)$$

Substituting these into (1.75) yields

$$lc = -\mu \frac{\int_c \pm \frac{1}{\eta} (\vec{a}_z \times \vec{\mathcal{E}}_t^\pm) \cdot \vec{a}_n dl}{\oint_{c'} \vec{\mathcal{H}}_t^\pm \cdot d\vec{l}'} \varepsilon \frac{\oint \mp \eta (\vec{a}_z \times \vec{\mathcal{H}}_t^\pm) \cdot \vec{a}_n dl'}{-\int_c \vec{\mathcal{E}}_t^\pm \cdot d\vec{l}} \quad (1.77)$$

From Figure 1.10 (replacing  $\vec{\mathcal{E}}_t$  with  $\vec{\mathcal{H}}_t$  and vice versa) we obtain the identities

$$(\vec{a}_z \times \vec{\mathcal{E}}_t^\pm) \cdot \vec{a}_n dl = \vec{\mathcal{E}}_t^\pm \cdot d\vec{l} \quad (1.78a)$$

and

$$(\vec{a}_z \times \vec{\mathcal{H}}_t^\pm) \cdot \vec{a}_n dl' = -\vec{\mathcal{H}}_t^\pm \cdot d\vec{l}' \quad (1.78b)$$

Substituting these into (1.77) yields

$$\begin{aligned} lc &= -\mu \frac{\pm \int_c \vec{\mathcal{E}}_t^\pm \cdot d\vec{l} \pm \oint \vec{\mathcal{H}}_t^\pm \cdot d\vec{l}'}{\oint_{c'} \vec{\mathcal{H}}_t^\pm \cdot d\vec{l}'} \varepsilon \frac{c'}{-\int_c \vec{\mathcal{E}}_t^\pm \cdot d\vec{l}} \\ &= \mu \varepsilon \end{aligned} \quad (1.79)$$

Taking the ratio of the basic definitions of  $g$  in (1.60) and  $c$  in (1.57) gives the relation  $g = (\sigma/\varepsilon)c$ . Substituting (1.79) into this gives the relation  $gl = \sigma\mu$ .

## 1.4 CLASSIFICATION OF TRANSMISSION LINES

One of the primary tasks in obtaining the complete solution for the voltage and current of a transmission line is the general solution of the transmission-line equations (Step 2). The type of line being considered significantly affects this solution. We are familiar with the difficulties in the solution of various ordinary differential equations encountered in the analysis of lumped circuits [A.2,A.5]. An example of an ordinary differential equation encountered in lumped-circuit analysis is

$$\frac{dV(t)}{dt} + aV(t) = b \sin(\omega t)$$

Although the equations to be solved for lumped systems are ordinary differential equations (there is only one independent variable, time  $t$ ) and are somewhat simpler to solve than the transmission-line equations, which are partial differential equations (since the voltage and current are functions of two independent variables, time  $t$  and position along the line  $z$ ), the type of circuit strongly affects the solution difficulty. For example, if any of the circuit elements are functions of time (a time-varying circuit), then the coefficients in the equation, for example,  $a$ , will be functions of the independent variable,  $t$ . An example is

$$\frac{dV(t)}{dt} + a(t)V(t) = b \sin(\omega t)$$

These equations, although linear, are said to be *nonconstant coefficient ordinary differential equations*, which are considerably more difficult to solve than constant coefficient ones [A.4]. Suppose one or more of the circuit elements are *nonlinear*; that is, the element voltage has a nonlinear relation to its current. In this case, the circuit differential equations become *nonlinear ordinary differential equations*, which are equally difficult to solve [A.4]. So the class of lumped circuit being considered drastically affects the difficulty of solution of the governing differential equations.

#### 1.4.1 Uniform versus Nonuniform Lines

Solution of the transmission-line partial differential equations has similar parallels. We have been implicitly assuming that the per-unit-length parameters are independent of position along the line  $z$  and, of course, time  $t$ . The per-unit-length parameters contain all the cross-sectional structural dimensions of the line. If the cross-sectional dimensions of the line vary along the line axis, then the per-unit-length parameters will be functions of the position variable,  $z$ , for example,  $g(z)$ ,  $c(z)$ , and  $l(z)$ . This makes the resulting transmission-line equations very difficult to solve because the coefficients, the per-unit-length parameters, will be functions of one of the independent variables in the same fashion as a nonconstant coefficient ordinary differential equation:

$$\frac{\partial V(z, t)}{\partial z} = -l(z) \frac{\partial I(z, t)}{\partial t}$$

$$\frac{\partial I(z, t)}{\partial z} = -g(z)V(z, t) - c(z) \frac{\partial V(z, t)}{\partial t}$$

Such transmission-line structures are said to be *nonuniform lines*. This includes both the cross-sectional dimensions of the line conductors and the cross-sectional dimensions of any inhomogeneous surrounding medium. If the cross-sectional dimensions of both the line conductors and the surrounding, perhaps inhomogeneous, medium are *constant along the line axis*, the line is said to be a *uniform line* whose resulting differential equations are simple to solve because the per-unit-length parameters  $l$ ,  $c$ , and  $g$  are constants independent of  $z$ . An example of a nonuniform (in conductor cross

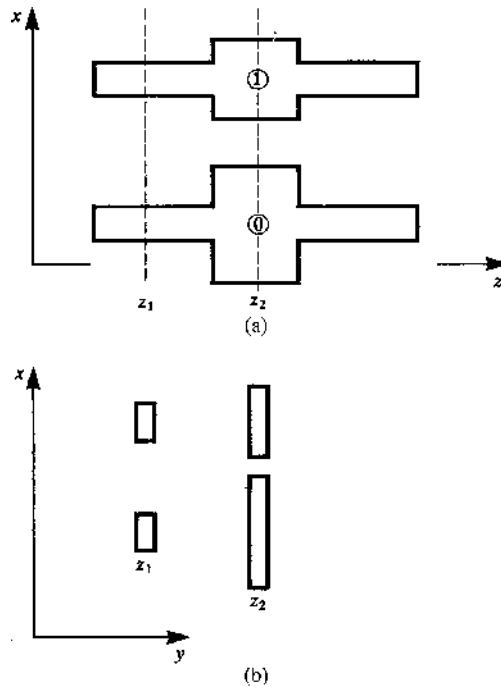


**FIGURE 1.11** Illustration of a nonuniform line caused by variations in the conductor cross section.

section) line is shown in Figure 1.11. Figure 1.11(a) shows the view along the line axis, whereas Figure 1.11(b) shows the view in cross section. Because the conductor cross sections are different at  $z_1$  and  $z_2$ , the per-unit-length parameters will be functions of position  $z$ . This type of structure occurs frequently on printed circuit boards. A common way of handling this is to divide the line into three uniform sections and cascade the representations. This is an approximation since it neglects the fringing of the fields at the junctions. Figure 1.12 shows a nonuniform line where the nonuniformity is introduced by the inhomogeneous medium. A wire is surrounded by dielectric insulation. Along the two end segments, the medium is inhomogeneous since in one part of the region the fields exist in the dielectric insulation,  $\epsilon_1, \mu_0$ , and in the other they exist in free space,  $\epsilon_0, \mu_0$ . In the middle region, the dielectric insulation is also inhomogeneous consisting of regions containing  $\epsilon_1, \mu_0, \epsilon_2, \mu_0$  and  $\epsilon_0, \mu_0$ . However, because of this change in the properties of the surrounding medium from one section to the next, the total line is a *nonuniform* one and the resulting per-unit-length parameters will be functions of  $z$ . The resulting transmission-line equations for Figures 1.11 and 1.12 are very difficult to solve because of the nonuniformity of the line. Again, a common way of analyzing this type of problem is to partition the line into a cascade of uniform subsections. This is, again, an approximation since it neglects the fringing of the fields at the junctions.

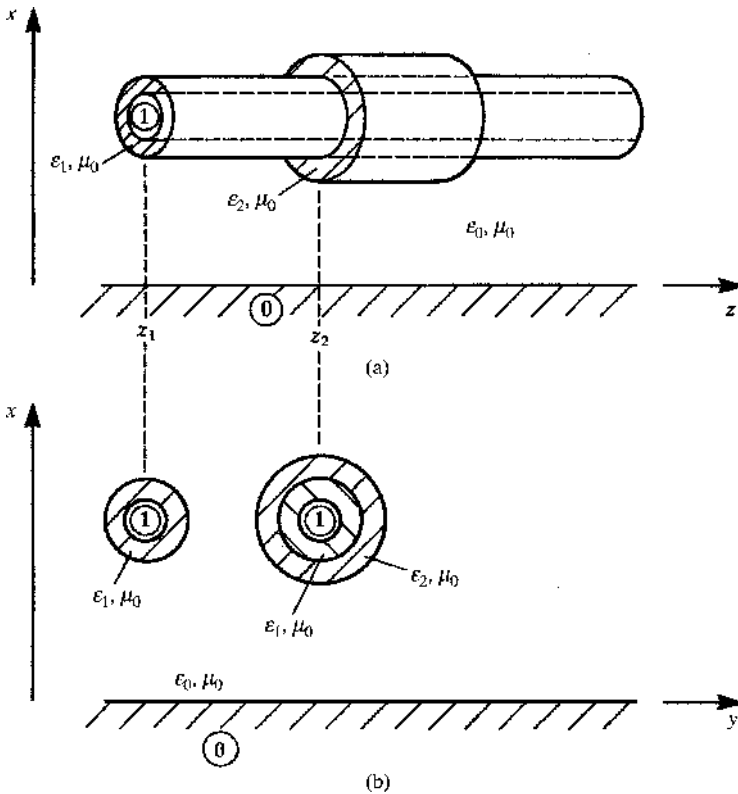


**FIGURE 1.12** Illustration of a nonuniform line caused by variations in the surrounding medium cross section.

#### 1.4.2 Homogeneous versus Inhomogeneous Surrounding Media

Figure 1.1 shows lines in a homogeneous medium; that is, there is one dielectric surrounding the conductors and hence the permittivity, conductivity, and permeability are independent of position in the space surrounding the conductors. Dielectric insulations surrounding wires such as in ribbon cables are examples of inhomogeneous media since the electric field lines will be partly in this dielectric insulation and partly in the remaining free space. The PCB structures in Figure 1.2(b) and (c) are also examples of lines in an inhomogeneous medium. The electric field lines will lie partly in the dielectric substrate and partly in the remaining free space. For structures in a homogeneous medium such as the wire-type structures in Figure 1.1 and the coupled stripline in Figure 1.2(a), all waves will travel at the same velocity. For lines consisting of  $n + 1$  conductors in an inhomogeneous medium, there will be  $n$  waves each traveling with different velocities. This complicates the solution of the transmission-line equations as we will see later.

There are numerous combinations of these characterizations. A line may be in a homogeneous medium yet because of a change in the conductor cross sections along the line, it would be classified as a nonuniform line and would be very difficult to solve. A line may be in an inhomogeneous medium but because this inhomogeneity as well as the conductor cross sections do not change along the line axis, it would be classified as a uniform line. It would be relatively simple to solve. For these reasons, we will restrict the transmission lines that we will consider in this text to be *uniform lines*. They may, however, be in a *homogeneous or an inhomogeneous medium*. In either case, a *uniform line* has (a) conductor cross sections that do not vary with  $z$  and (b) surrounding dielectric properties that may be functions of  $x$  and  $y$  but do not vary with  $z$ .

Technically, an inhomogeneous surrounding medium, although uniform along the line ( $z$ ) axis, invalidates the basic assumption of a TEM field structure. The reason for this is that a TEM field structure must have one and only one velocity of propagation of the waves in the medium. However, this cannot be the case for an inhomogeneous medium. If one portion of the inhomogeneous medium is characterized by  $\epsilon_1, \mu_0$  and the other is characterized by  $\epsilon_2, \mu_0$ , such as for the lines in Figure 1.2(b) and (c), the velocities of TEM waves in infinite, homogeneous regions characterized by these parameters will be  $v_1 = 1/\sqrt{\epsilon_1\mu_0}$  and  $v_2 = 1/\sqrt{\epsilon_2\mu_0}$ , which will be different. Nevertheless, the transmission-line equations are usually solved in spite of this observation and are assumed to adequately represent the situation so long as these velocities are not substantially different. This is referred to as the *quasi-TEM assumption*.

### 1.4.3 Lossless versus Lossy Lines

All of the previous derivations include losses in the medium through a per-unit-length conductance parameter  $g$ . This loss in the surrounding (assumed homogeneous) medium does not invalidate the TEM field structure assumption. However, the previous derivations also assumed *perfect conductors*. In other words, the conductors were assumed to be lossless and to have no resistance properties along their  $z$  axes. Practical transmission lines are obviously constructed of imperfect conductors that have loss. However, in order that the transmission line be a useful guided wave structure, these conductor losses must be small. Nevertheless, how shall we include these losses and what will be their effect on the ideal assumption of a TEM field structure?

We may include the possibility of the line conductors being *imperfect conductors* with small losses through a per-unit-length resistance parameter  $r$ . Unlike losses in the surrounding medium, *lossy conductors implicitly invalidate the TEM field structure assumption*. Figure 1.13 shows why this is the case. The line current flowing through the imperfect line conductor generates a nonzero electric field along the conductor surface,  $\mathcal{E}_z(z, t) = rI(z, t)$ , which is directed in the  $z$  direction, thereby violating the basic assumption of the TEM field structure in the surrounding medium. The total electric field is the sum of the transverse component and this  $z$ -directed component.

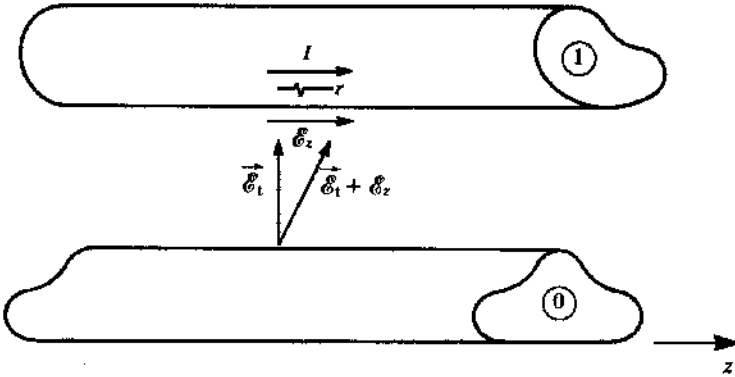


FIGURE 1.13 Illustration of the effect of conductor losses in creating non-TEM fields.

However, if the conductor losses are small, this resulting field structure is *almost similar to a TEM structure*. This is again referred to as the *quasi-TEM assumption* and, although the transmission-line equations are no longer valid, they are nevertheless assumed to represent the situation for small losses through the inclusion of the per-unit-length resistance parameter  $r$ . In the derivation of the transmission-line equations for an MTL, we will include this parameter.

In summary, the TEM field structure and mode of propagation characterization of a transmission line is valid only for uniform lines consisting of perfect conductors and surrounded by a homogeneous medium. Note that this medium may be lossy and not violate the TEM assumption so long as it is homogeneous (in  $\sigma$ ,  $\epsilon$ , and  $\mu$ ). Violations of these assumptions (lossy conductors and/or an inhomogeneous medium surrounding the conductors) are considered under the *quasi-TEM* assumption so long as they are not extreme [17, 18].

### 1.5 RESTRICTIONS ON THE APPLICABILITY OF THE TRANSMISSION-LINE EQUATION FORMULATION

There are some additional, implicit assumptions in the TEM transmission-line equation characterization. In the derivation of the transmission-line equations from the distributed-parameter lumped circuit of Figure 1.8, distributing the lumped elements along the line and allowing the section length to go to zero,  $\lim_{\Delta z \rightarrow 0} \Delta z$ , means that line lengths that are *electrically long*, that is, much greater than a wavelength  $\lambda$ , are properly handled with this lumped-circuit characterization. However, it was assumed that the line cross-sectional dimensions such as conductor separations were electrically small at the frequencies of excitation of the line. Structures whose cross-sectional dimensions are electrically large at the frequency of excitation will have, in addition to the TEM field structure and mode of propagation, other higher order

TE and TM field structures and modes of propagation simultaneously with the TEM mode [A.1,17–19]. Therefore, the solution of the transmission-line equations does not give the complete solution in the range of frequencies where these non-TEM modes coexist on the line. A comparison of the predictions of the TEM transmission-line equation results with the results of a numerical code (which does not presuppose existence of only the TEM mode) for a two-wire line showed differences beginning with frequencies where the wire separations were as small as  $\lambda/40$  [H.7]. Analytical solution of Maxwell's equations in order to consider the total effect of all modes is usually a formidable task. There are certain structures where an analytical solution is feasible, and we will discuss these in the next two sections.

### 1.5.1 Higher Order Modes

In the following two subsections, we analytically solve Maxwell's equations for two *closed structures* to obtain the complete solution and demonstrate that the TEM formulation is complete up to some frequency where the conductor separations are some significant fraction of a wavelength above which higher order modes begin to propagate.

**1.5.1.1 The Infinite, Parallel-Plate Transmission Line** Consider the *infinite, parallel-plate transmission line* shown in Figure 1.14. The two infinite and perfectly conducting plates lie in the  $y$ - $z$  plane and are located at  $x = 0$  and  $x = a$ . We will obtain the complete solutions for the fields in the space between the two plates, which is assumed to be homogeneous and lossless and characterized by  $\varepsilon$  and  $\mu$ . Maxwell's equations for sinusoidal excitation become

$$\nabla \times \vec{E} = -j\omega\mu\vec{H} \quad (1.80a)$$

$$\nabla \times \vec{H} = j\omega\varepsilon\vec{E} \quad (1.80b)$$

Expanding these and noting that the plates are infinite in extent in the  $y$  direction so that  $\frac{\partial}{\partial y} = 0$  gives [A.1]

$$\begin{aligned} \frac{\partial E_y}{\partial z} &= j\omega\mu H_x \\ \frac{\partial E_x}{\partial z} - \frac{\partial E_z}{\partial x} &= -j\omega\mu H_y \\ \frac{\partial E_y}{\partial x} &= -j\omega\mu H_z \\ \frac{\partial H_y}{\partial z} &= -j\omega\varepsilon E_x \\ \frac{\partial H_x}{\partial z} - \frac{\partial H_z}{\partial x} &= j\omega\varepsilon E_y \\ \frac{\partial H_y}{\partial x} &= j\omega\varepsilon E_z \end{aligned} \quad (1.81)$$

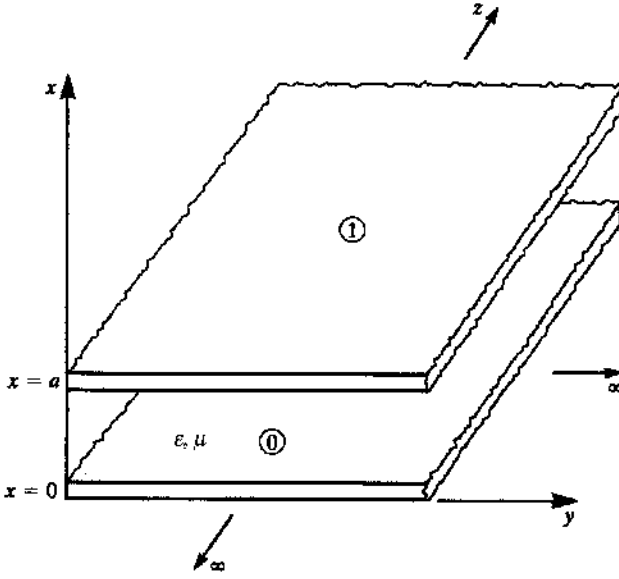


**FIGURE 1.14** The infinite parallel-plate waveguide for demonstrating the effect of cross-sectional dimensions on higher order modes.

In addition, we have the *wave equations* [A.1]:

$$\begin{aligned} \nabla^2 \vec{E} + \omega^2 \mu \epsilon \vec{E} &= 0 \\ \nabla^2 \vec{H} + \omega^2 \mu \epsilon \vec{H} &= 0 \end{aligned} \tag{1.82}$$

Expanding these and recalling that the plates are infinite in the *y* dimension so that  $\frac{\partial}{\partial y} = 0$  gives [A.1]

$$\begin{aligned} \frac{\partial^2 \vec{E}}{\partial x^2} + \frac{\partial^2 \vec{E}}{\partial z^2} + \omega^2 \mu \epsilon \vec{E} &= 0 \\ \frac{\partial^2 \vec{H}}{\partial x^2} + \frac{\partial^2 \vec{H}}{\partial z^2} + \omega^2 \mu \epsilon \vec{H} &= 0 \end{aligned} \tag{1.83}$$

Let us now look for waves propagating in the *+z* direction. To do so, we use the principle of *separation of variables*, where we separate the dependence on *x*, *y*, and *z* as

$$\vec{E}(x, y, z) = \vec{E}'(x, y)e^{-\gamma z} \tag{1.84}$$

where  $\gamma$  is the propagation constant (to be determined). Substituting this into (1.81) yields

$$\begin{aligned}
 \gamma E'_y &= -j\omega\mu H'_x \\
 -\gamma E'_x - \frac{\partial E'_z}{\partial x} &= -j\omega\mu H'_y \\
 \frac{\partial E'_y}{\partial x} &= -j\omega\mu H'_z \\
 \gamma H'_y &= j\omega\varepsilon E'_x \\
 -\gamma H'_x - \frac{\partial H'_z}{\partial x} &= j\omega\varepsilon E'_y \\
 \frac{\partial H'_y}{\partial x} &= j\omega\varepsilon E'_z
 \end{aligned} \tag{1.85}$$

and

$$\begin{aligned}
 \frac{\partial^2 \vec{E}'}{\partial x^2} + (\gamma^2 + \omega^2\mu\varepsilon)\vec{E}' &= 0 \\
 \frac{\partial^2 \vec{H}'}{\partial x^2} + (\gamma^2 + \omega^2\mu\varepsilon)\vec{H}' &= 0
 \end{aligned} \tag{1.86}$$

The equations in (1.85) can be manipulated to yield [A.1]

$$\begin{aligned}
 H'_x &= -\frac{\gamma}{h^2} \frac{\partial H'_z}{\partial x} \\
 E'_x &= -\frac{\gamma}{h^2} \frac{\partial E'_z}{\partial x} \\
 H'_y &= -\frac{j\omega\varepsilon}{h^2} \frac{\partial E'_z}{\partial x} \\
 E'_y &= \frac{j\omega\mu}{h^2} \frac{\partial H'_z}{\partial x} \\
 h^2 &= \gamma^2 + \omega^2\mu\varepsilon
 \end{aligned} \tag{1.87}$$

Observe that  $E'(x, y)$  and  $H'(x, y)$  are functions of  $x$  only since there can be no variation in the  $y$  direction due to the infinite extent of the plates in this direction and also the  $z$  variation has been assumed. Thus the partial derivatives in (1.85)–(1.87) can be replaced by ordinary derivatives. We now investigate the various modes of propagation.

*The Transverse Electric (TE) Mode ( $E_z = 0$ )* The TE mode of propagation assumes that the electric field is confined to the transverse or  $x$ – $y$  plane so that  $E_z = 0$ . Therefore, from (1.87) we see that  $E'_x = H'_y = 0$ . The wave equations in (1.86) reduce to

$$\frac{d^2 E'_y}{dx^2} + h^2 E'_y = 0 \tag{1.88}$$

whose general solution is

$$E'_y = C_1 \sin(hx) + C_2 \cos(hx) \quad (1.89)$$

The boundary conditions are such that the electric field tangent to the surfaces of the plates is zero:

$$E_y = 0|_{x=0, x=a} \quad (1.90)$$

which, when applied to (1.89), yields  $C_2 = 0$  and  $ha = m$  for  $m = 0, 1, 2, 3, \dots$ . Thus, the solution becomes

$$E_y = C_1 \sin\left(\frac{m\pi x}{a}\right) e^{-\gamma z} \quad (1.91)$$

From (1.85) we obtain

$$\begin{aligned} H_z &= j \frac{1}{\omega\mu} \frac{\partial E_y}{\partial x} \\ &= j \frac{m\pi}{\omega\mu a} C_1 \cos\left(\frac{m\pi x}{a}\right) e^{-\gamma z} \end{aligned} \quad (1.92)$$

and

$$H_x = j \frac{\gamma}{\omega\mu} C_1 \sin\left(\frac{m\pi x}{a}\right) e^{-\gamma z} \quad (1.93)$$

Since

$$h = \frac{m\pi}{a} \quad (1.94)$$

the propagation constant becomes

$$\gamma = \sqrt{\left(\frac{m\pi}{a}\right)^2 - \omega^2 \mu \varepsilon} \quad (1.95)$$

For the lowest order mode,  $m = 0$ , all field components vanish. The next higher order mode is the  $TE_1$  mode for  $m = 1$ .

*The Transverse Magnetic (TM) Mode ( $H_z = 0$ )* The TM mode has the magnetic field confined to the transverse  $x$ - $y$  plane so that  $H_z = 0$ . Carrying through a development similar to the above for this mode gives the nonzero field vectors as

$$\begin{aligned} H_y &= D_2 \cos\left(\frac{n\pi x}{a}\right) e^{-\gamma z} \\ E_x &= -j \frac{\gamma}{\omega\varepsilon} D_2 \cos\left(\frac{n\pi x}{a}\right) e^{-\gamma z} \\ E_z &= j \frac{n\pi}{a\omega\varepsilon} D_2 \sin\left(\frac{n\pi x}{a}\right) e^{-\gamma z} \end{aligned} \quad (1.96)$$

for  $n = 0, 1, 2, \dots$ . The propagation constant is again given by (1.95) with  $m$  replaced by  $n$ . In contrast to the TE modes, the lowest order TM mode is the  $\text{TM}_0$  mode for  $n = 0$ . For this case, the propagation constant reduces to the familiar

$$\begin{aligned}\gamma &= j\omega\sqrt{\mu\varepsilon} \\ &= j\beta\end{aligned}\tag{1.97}$$

and the field vectors in (1.96) reduce to

$$\begin{aligned}H_y &= D_2 e^{-j\beta z} \\ E_x &= -j \frac{\gamma}{\omega\varepsilon} D_2 e^{-j\beta z} \\ &= \sqrt{\frac{\mu}{\varepsilon}} D_2 e^{-j\beta z} \\ E_z &= 0\end{aligned}\tag{1.98}$$

However, this is the TEM mode!

The transmission-line equations for this TEM mode can be obtained by differentiating (1.98) with respect to  $z$  to yield

$$\begin{aligned}\frac{dE_x}{dz} &= -j\omega\mu H_y \\ \frac{dH_y}{dz} &= -j\omega\varepsilon E_x\end{aligned}\tag{1.99}$$

We may write these in terms of voltage and current by integrating in the transverse plane:

$$\begin{aligned}V(z) &= -\int_{x=0}^{x=a} E_x dx \\ &= -aE_x\end{aligned}\tag{1.100a}$$

and

$$I(z) = -wH_y\tag{1.100b}$$

The result for the current in (1.100b) is due to the fact that the  $H$  field is tangent to the upper and lower plates that are assumed to be perfect conductors and hence produces a surface current on the plate  $J_{sz} = -H_y|_{x=a}$  in A/m that is directed in the  $z$  direction. In a section of width  $w$  along the  $y$  dimension, the total current is  $J_{sz}w = -H_yw$  A.

Hence (1.99) becomes

$$\begin{aligned}\frac{dV}{dz} &= j\omega\mu \int_{x=0}^{x=a} H_y dx \\ &= -j\omega \underbrace{\left(\mu \frac{a}{w}\right)}_l \underbrace{(-H_y w)}_I \\ \frac{dI}{dz} &= -j\omega \underbrace{\left(\varepsilon \frac{w}{a}\right)}_c V\end{aligned}\tag{1.101}$$

and the per-unit-length inductance and capacitance are then defined as

$$\begin{aligned}l &= \mu \frac{a}{w} \quad \text{H/m} \\ c &= \varepsilon \frac{w}{a} \quad \text{F/m}\end{aligned}\tag{1.102}$$

Therefore, the lowest order TM mode,  $\text{TM}_0$ , is equivalent to the TEM mode and the  $\text{TE}_0$  mode is nonexistent. We must then ascertain when the next higher order modes begin to propagate, thus adding to the total picture. The propagation constant in (1.95) must be imaginary or at least have a nonzero imaginary part. Clearly, for  $m = n = 0$ , we have the propagation constant of a plane wave:  $\gamma = j\omega\sqrt{\mu\varepsilon} = j\beta$ . For higher order modes to propagate, we require from (1.95) that  $\omega^2\mu\varepsilon \geq h^2$ , giving

$$\omega \geq \frac{1}{\sqrt{\mu\varepsilon}} \frac{n\pi}{a}\tag{1.103}$$

The cutoff frequency for the lowest order TEM mode,  $\text{TM}_0$ , is clearly dc. The cutoff frequencies of the next higher order modes,  $\text{TE}_1$  and  $\text{TM}_1$ , are from (1.103)

$$\begin{aligned}f_{\text{TE}_1, \text{TM}_1} &= \frac{1}{2\pi\sqrt{\mu\varepsilon}} \frac{\pi}{a} \\ &= \frac{v}{2a}\end{aligned}\tag{1.104}$$

In terms of wavelength,  $\lambda = v/f$ , we find that the TEM mode will be the only possible mode so long as the plate separation  $a$  is less than one-half wavelength, that is,

$$a < \frac{\lambda}{2}\tag{1.105}$$

This illustrates that so long as the cross-sectional dimensions of the line are electrically small, only the TEM mode can propagate! This is illustrated in Figure 1.15.

**1.5.1.2 The Coaxial Transmission Line** Another *closed system* transmission line that is capable of supporting the TEM mode is the *coaxial transmission line* shown in

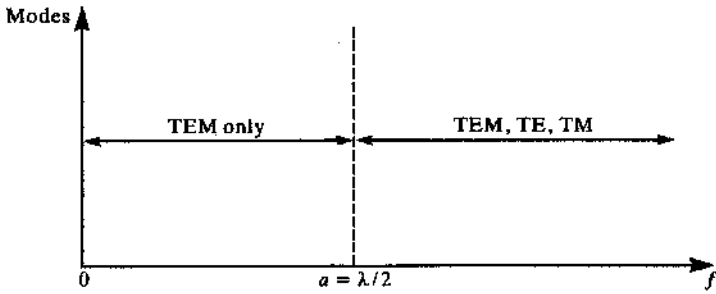


**FIGURE 1.15** Illustration of the dependence of higher order modes on cross-sectional electrical dimensions for the parallel-plate transmission line.

Figure 1.16. The general solution to Maxwell’s equations for the fields and modes in the space between the inner wire and the outer shield was obtained in [1]. Clearly, this structure can support the TEM mode with a cutoff frequency of dc. The higher order TE and TM modes have the following cutoff properties. The lowest order TE mode is cutoff for frequencies such that the average circumference between the conductors is less than approximately a wavelength, that is,

$$2\pi \frac{(a + b)}{2} < \lambda \tag{1.106}$$

Similarly, the lowest order TM mode is cutoff for frequencies such that the difference between the two conductor radii is less than approximately one-half wavelength, that is,

$$(b - a) < \frac{\lambda}{2} \tag{1.107}$$

These results again support the notion that the TEM mode will be the only mode of propagation in closed systems so long as the conductor separation is electrically small.

**1.5.1.3 Two-Wire Lines** The previous two transmission-line structures are closed systems. For *open systems* such as the two-wire line, the issue of higher order modes is not so clear-cut. Numerical analysis of a two-wire line given in [H.7] showed that the predictions of the transmission-line formulation for the two-wire line began



**FIGURE 1.16** The coaxial cable for illustrating the dependence of higher order modes on cross-sectional electrical dimensions.

to deviate from the complete solution when the cross-sectional dimensions such as wire separation are no longer electrically small. This supports our intuition. The problem was investigated in more detail in [19] where these notions are confirmed. Also certain other modes are capable of propagating with no clearly defined cutoff frequency. However, the TEM mode formulation and the resulting transmission-line equation representation for two-wire lines will be reasonably adequate so long as the wire separations are electrically small. Ordinarily, this is satisfied for practical transmission-line structures.

### 1.5.2 Transmission-Line Currents versus Antenna Currents

There is one remaining restriction on the completeness of the TEM mode, transmission-line representation that needs to be discussed. It can be shown that under the TEM transmission-line equation formulation for a two-conductor line, the currents so determined on the two conductors at any cross section must be equal in magnitude and oppositely directed (see Problem 1.3). Thus, the total current at any cross section is zero. This is the origin of the reference to the term that one of the conductors serves as a “return” for the current on the other conductor. On a transmission line, there may also be currents that do not sum to zero at any cross section. These so-called “antenna currents” or “common-mode currents” tend to go to zero at the line endpoints. Hence, their presence along the line does not substantially change the predictions of the terminal voltages and currents. Therefore, in the usual use of the transmission-line model to predict crosstalk and signal integrity on transmission lines, the TEM transmission-line equations give substantially the complete result.

Consider the pair of parallel wires shown in Figure 1.17(a) carrying, at the same cross section, currents  $I_1$  and  $I_2$ . In general, we may decompose or represent these as a linear combination of two other currents. The so-called *differential-mode currents*  $I_D$  are equal in magnitude at a cross section and are oppositely directed, as shown in Figure 1.17(b). These correspond to the TEM mode, transmission-line currents that will be predicted by the transmission-line model. The other currents are the so-called *common-mode currents*  $I_C$  which are equal in magnitude at a cross section but are directed in the same direction, as shown in Figure 1.17(c). These are sometimes referred to as “antenna-mode” currents [20, 21]. This decomposition can be obtained by writing, from Figure 1.17,

$$\begin{aligned} I_1 &= I_C + I_D \\ I_2 &= I_C - I_D \end{aligned} \tag{1.108}$$

In matrix form, these can be written as

$$\begin{bmatrix} I_1 \\ I_2 \end{bmatrix} = \begin{bmatrix} 1 & 1 \\ 1 & -1 \end{bmatrix} \begin{bmatrix} I_C \\ I_D \end{bmatrix} \tag{1.109}$$

Equation (1.109) represents a nonsingular transformation between the two sets of currents since the transformation matrix is nonsingular. Therefore, its inverse can be

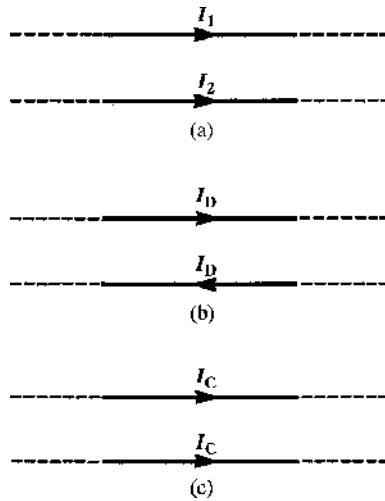


**FIGURE 1.17** Illustration of the decomposition of total currents into differential-mode (transmission-line mode) and common-mode (antenna mode) components.

taken and the transformation reversed to yield

$$\begin{bmatrix} I_C \\ I_D \end{bmatrix} = \frac{1}{2} \begin{bmatrix} 1 & 1 \\ 1 & -1 \end{bmatrix} \begin{bmatrix} I_1 \\ I_2 \end{bmatrix} \quad (1.110)$$

This gives

$$\begin{aligned} I_C &= \frac{I_1 + I_2}{2} \\ I_D &= \frac{I_1 - I_2}{2} \end{aligned} \quad (1.111)$$

Note that  $I_2 \cong -I_1$ ; that is, in a normal situation, one current “returns” to its source on the other conductor. Hence,  $I_C \ll I_D$ . Therefore, the common-mode currents are much smaller in magnitude than the differential-mode currents and so do not substantially affect the results of an analysis of currents and voltages of a transmission line. However, in the prediction of radiated emissions from this two-wire line, the common-mode currents are significant because the radiated electric fields from the differential-mode currents tend to subtract, but those from the common-mode currents tend to add. Thus, a “small” common-mode current can give the same order of magnitude of radiated emission as a much larger differential-mode current. This was confirmed for cables and PCBs in [A.3,22,23]. The significant point here is that if one bases a prediction of the *radiated emissions* from a two-conductor line on the currents obtained from a transmission-line equation analysis, the predicted emissions will generally lie far below those of the emissions due to the common-mode currents. On the contrary, the common-mode currents can generally be ignored in a near-field transmission-line analysis such as in determining *crossstalk*.

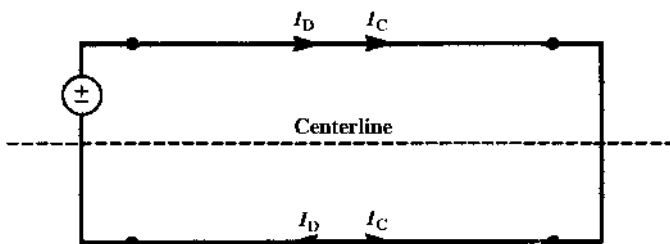


FIGURE 1.18 Illustration of an asymmetry that creates common-mode currents.

There are a number of ways through which these non-TEM mode currents can be created on a transmission line. Figure 1.18 illustrates one of these. It is important to remember that the TEM mode, transmission-line equation formulation only characterizes the line and assumes that the two (or more) conductors of the line continue indefinitely along the  $z$  axis. The analysis does not inherently consider the field effects of the eventual terminations for a finite-length line. This problem was investigated in [24]. It was found that *asymmetries* as well as the presence of nearby metallic structures create these “nonideal” currents. For example, consider the two-wire line shown in Figure 1.18, which is driven by a voltage source at the left end and terminated in a short circuit at the right end. This was analyzed using a numerical solution of Maxwell’s equations, commonly referred to as a method of moments (MoM). This analysis gives the complete solution for the currents without presupposing the existence of only the TEM mode. It was found that if the voltage source was situated and modeled as being centered in the left segment on the centerline, then  $I_2 = -I_1$ ; in other words, the currents on the wires are only differential-mode currents. However, if the voltage source was placed asymmetrically to the centerline such as shown and the resulting currents decomposed as in (1.111), common-mode currents appeared. This asymmetrical placement of the source, which is not explicitly considered in the transmission-line equation formulation, was apparently the source.

The important point here is that the TEM mode, transmission-line equation formulation that we will consider in this text predicts only the differential-mode currents. If the line cross section is electrically small and one is interested only in predicting the currents and voltages on the line for the purposes of predicting signal distortion and *crossstalk* (the primary goal of this text), this prediction will be reasonably accurate. On the contrary, if one is interested in predicting the radiated electric field from this line, then the predictions of that field using only the currents predicted by the transmission-line equation formulation will most likely be inadequate since the contributions due to the common-mode currents typically are frequently the dominant contributors to radiated emissions [22, 23].

## 1.6 THE TIME DOMAIN VERSUS THE FREQUENCY DOMAIN

The two important domains that we will use throughout this text to analyze transmission-line structures are the *time domain* and the *frequency domain*. It is

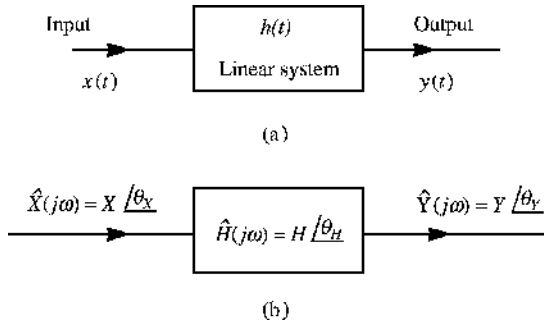


**FIGURE 1.19** Illustration of the concept of a transfer function for a linear system.

critically important that we understand these two notions since they will form the heart of our analyses. First, let us discuss viewing the transmission-line problem as a *single-input, single-output* system as illustrated in Figure 1.19(a). This is a very standard way of viewing a system [A.2,A.5]. An input  $x(t)$  is applied to the system (which we suppose here is a linear one) and produces the output  $y(t)$ . The system may be characterized by its *impulse response*  $h(t)$ . Analysis in the *time domain* refers to applying a signal or waveform that has some general shape and dependence on time  $t$  and determining the output or solution as a general waveform  $y(t)$ . Although not strictly required, we may obtain this solution in terms of the impulse response  $h(t)$ . The impulse response is the response when a unit impulse function is applied at the input; that is, if  $x(t) = \delta(t)$ , then  $y(t) = h(t)$ . The *time-domain solution* may be obtained with the *convolution integral* [A.2,A.5]:

$$y(t) = \int_0^t h(t - \tau)x(\tau)d\tau \quad (1.112)$$

Analysis in the *frequency domain* refers to applying a single-frequency sinusoidal waveform

$$x(t) = X \cos(\omega t + \theta_X) \quad (1.113)$$

and determining the output under the assumption that the system response has reached *steady state*. For a linear system, the response will be of the same form and the same frequency as the input signal but with a different amplitude and phase:

$$y(t) = Y \cos(\omega t + \theta_Y) \quad (1.114)$$

To analyze the response of the system, we move to the frequency domain by replacing time quantities with their complex-valued *phasor* equivalents [A.2,A.5]:

$$x(t) = X \cos(\omega t + \theta_X) \Rightarrow \hat{X}(j\omega) = X \angle \theta_X \quad (1.115a)$$

$$y(t) = Y \cos(\omega t + \theta_Y) \Rightarrow \hat{Y}(j\omega) = Y \angle \theta_Y \quad (1.115b)$$

as illustrated in Figure 1.19(b), and we write all complex-valued quantities with a caret ( $\hat{\cdot}$ ) over them and  $j = \sqrt{-1}$ . The impulse response in the frequency domain is the familiar *transfer function* or *frequency response* that also has a magnitude and a phase:

$$h(t) \Rightarrow \hat{H}(j\omega) = H \angle \theta_H \quad (1.115c)$$

In order to obtain this frequency response, we apply a unit amplitude, zero phase input sinusoidal signal, sweep its frequency, and determine the response magnitude and phase at each applied frequency:

$$\hat{X} = 1 \angle 0^\circ \Rightarrow \hat{Y} = H \angle \theta_H \quad (1.116)$$

Then the solution process in the *frequency domain* is to obtain the magnitude and phase of the output using complex algebra as

$$Y \angle \theta_Y = H \angle \theta_H \times X \angle \theta_X \quad (1.117)$$

The result is obtained by multiplying magnitudes and adding angles in accordance with the rules of complex arithmetic [A.2,A.5]:

$$\hat{Y} = (HX) \angle (\theta_H + \theta_X) \quad (1.118)$$

Having done this, we return to the *time domain* by (a) multiplying the phasor result by  $e^{j\omega t}$  and (b) taking the real part of the result:

$$\begin{aligned} y(t) &= \text{Re}\{\hat{Y}e^{j\omega t}\} \\ &= HX \cos(\omega t + \theta_H + \theta_X) \end{aligned} \quad (1.119)$$

This phasor analysis method is virtually the heart of all analyses of electrical engineering systems as well as other dynamical systems.

We may represent a two-conductor transmission-line problem in the form of a single-input, single-output system as shown in Figure 1.20. Consider a general source and load termination of a transmission line shown in Figure 1.20(a). The source consists of an open-circuit voltage source,  $V_S(t)$ , and a source resistance,  $R_S$ . The load represents, perhaps, the input to a device and is represented by the resistor  $R_L$ . We may be interested in determining, for example, the output voltage across the load,  $V_{\text{out}}(t)$ . In order to put this into the form of a single-input, single-output system as illustrated in Figure 1.19(a), we consider the input to the system to be the voltage source,  $x(t) = V_S(t)$ , and the output to be the voltage across the load resistor,  $y(t) = V_{\text{out}}(t)$ . Hence we imbed the line and the termination resistors in the system as shown in Figure 1.20(b). It is very important to observe that the “system” contains the termination resistors. Hence, nonlinear terminations render the problem a nonlinear one, and the phasor solution method is no longer valid. In the case of a multiconductor

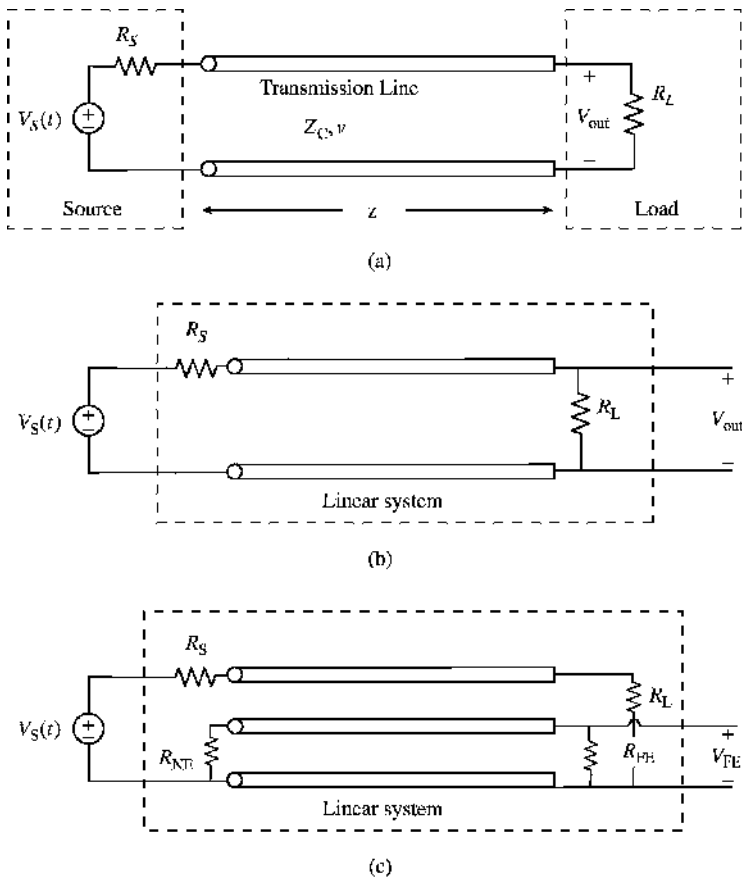


**FIGURE 1.20** Characterizing a transmission line as a single-input, single-output system.

line as shown in Figure 1.20(c), the input is again  $x(t) = V_S(t)$  and the desired output may be, for example, the far-end crosstalk voltage,  $y(t) = V_{FE}(t)$ .

### 1.6.1 The Fourier Series and Transform

The primary reason we concentrate so much emphasis on the single-frequency sinusoidal response of a linear system via the frequency domain is that we can decompose any periodic time-domain waveform into its sinusoidal components via the Fourier series [A.2,A.3]. Hence we can represent any periodic waveform having period  $P$  as the infinite sum of sinusoids whose frequencies are multiples of the basic repetition frequency

$$f_0 = \frac{1}{P} \tag{1.120}$$

as [A.2,A.3]

$$x(t) = c_0 + \sum_{n=1}^{\infty} 2c_n \cos(n\omega_0 t + \angle c_n) \quad (1.121)$$

and  $\omega_0 = 2\pi f_0 = 2\pi/P$ . The Fourier expansion coefficients in (1.121) are obtained from [A.2,A.3]

$$\begin{aligned} \hat{c}_n &= \frac{1}{P} \int_{t_1}^{t_1+P} x(t) e^{-jn\omega_0 t} dt \\ &= c_n \angle c_n \end{aligned} \quad (1.122)$$

where  $\hat{c}_n$  is a complex number, and  $c_n$  and  $\angle c_n$  are the magnitude and the phase, respectively, of it. In the frequency domain, we can determine the transfer function at each of these *harmonics* as

$$\hat{H}(jn\omega_0) = |\hat{H}(jn\omega_0)| \angle \hat{H}(jn\omega_0) \quad (1.123)$$

If the system (line and terminations) is linear, then we may employ *superposition* and pass each sinusoidal component of the input through the system and sum them at the output to obtain the Fourier series of the output  $y(t)$  as illustrated in Figure 1.21:

$$y(t) = c_0 \hat{H}(0) + \sum_{n=1}^{\infty} 2c_n |\hat{H}(jn\omega_0)| \cos(n\omega_0 t + \angle c_n + \angle \hat{H}(jn\omega_0)) \quad (1.124)$$

This is an incredibly powerful result. It says that we can indirectly solve for the time-domain response of the output  $y(t)$  by decomposing the input signal,  $x(t)$ , into its sinusoidal components with the Fourier series as in (1.121), solving for the frequency response of the system to these harmonics of the input signal, and then *summing these individual responses in time* as in (1.124). However, this will represent only the steady-state solution part of  $y(t)$  and transients are not included. Theoretically, the Fourier series requires an infinite number of harmonics be summed to yield the time-domain function. In a practical sense, we only need to sum a finite number to arrive at a reasonable approximation to the output solution  $y(t)$ .

For waveforms that are not periodic, that is, consist of a single pulse, the Fourier transform provides a similar representation [A.2,A.3]. In this case, the discrete spectrum consisting of harmonics is replaced by a continuous spectrum. The discrete Fourier series coefficients are replaced by the Fourier transform,  $\hat{X}(j\omega)$ . The process described above is essentially unchanged.

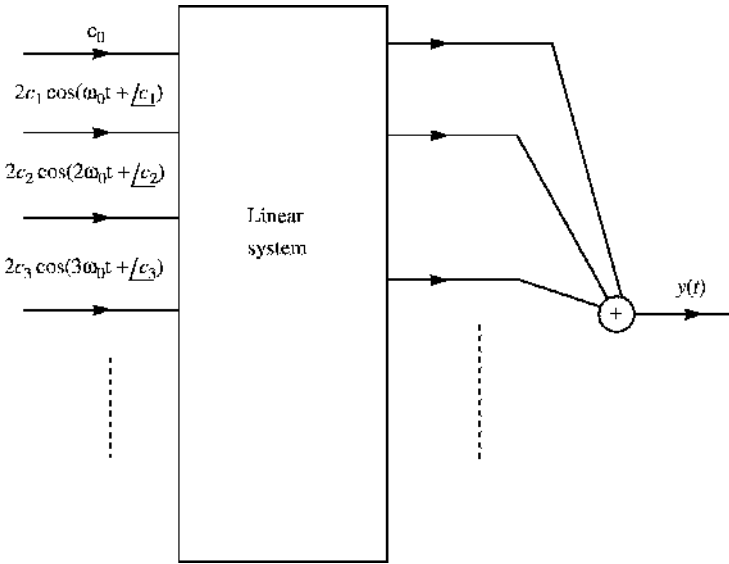


**FIGURE 1.21** Illustration of using superposition and the Fourier series to indirectly obtain the time-domain output of a linear system.

**1.6.2 Spectra and Bandwidth of Digital Waveforms**

The methods and techniques for analyzing MTLs discussed in this text apply for source waveforms in the termination networks as well as incident fields that have any general time variation. However, because of the preponderance of digital methods and devices today, we will concentrate our examples on digital waveforms that represent clock and data signals. A digital clock signal is periodic and has a trapezoidal waveform shown in Figure 1.22. The pulse width  $\tau$  is defined between the half-amplitude levels of the pulse, and  $\tau_r$  and  $\tau_f$  denote the 0–100 % rise and fall times of the pulse, respectively. The expansion coefficients in (1.122) were obtained in [A.3 ] and are

$$c_0 = A \frac{\tau}{P} \tag{1.125a}$$

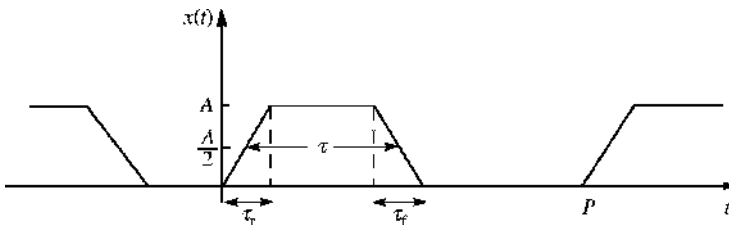


**FIGURE 1.22** A periodic, trapezoidal pulse train representing a digital signal.

$$\hat{c}_n = -j \frac{A}{2\pi n} \left( \frac{\sin\left(\frac{n\pi\tau_r}{P}\right)}{\frac{n\pi\tau_r}{P}} e^{jn\pi\tau/P} - \frac{\sin\left(\frac{n\pi\tau_f}{P}\right)}{\frac{n\pi\tau_f}{P}} e^{-jn\pi\tau/P} \right) e^{-jn\pi\frac{(\tau+\tau_r)}{P}} \quad (1.125b)$$

In digital applications, it is usually desired to have the rise and fall times of the pulse equal. In this case, the expansion coefficients simplify to [A.3]

$$\hat{c}_n = A \frac{\tau}{P} \frac{\sin\left(\frac{n\pi\tau}{P}\right)}{\frac{n\pi\tau}{P}} \frac{\sin\left(\frac{n\pi\tau_r}{P}\right)}{\frac{n\pi\tau_r}{P}} e^{-jn\pi\frac{(\tau+\tau_r)}{P}}, \quad \tau_r = \tau_f \quad (1.126)$$

Observe that the dc component,  $c_0$  in (1.125a), and the harmonic amplitudes involve the ratio of the pulse width to pulse period or the pulse *duty cycle*:

$$D = \frac{\tau}{P} \quad (1.127)$$

It is also generally desired to have the duty cycle to be 50 % or  $D = 0.5$ . Bounds on the spectral amplitudes can be developed for the case where the rise and fall times are equal [A.3]. These are shown in Figure 1.23. There are two break frequencies. Up to  $f = 1/\pi\tau = f_0/\pi D$ , the amplitudes are bounded by a 0 dB/decade slope and after that fall off at a rate of  $-20$  dB/decade. Above the next break frequency of  $f = 1/\pi\tau_r$ , the harmonic amplitudes fall off at a rate of  $-40$  dB/decade. Hence the high-frequency spectral content is primarily determined by the rise/fall times of the pulse.

This result can be derived for unequal rise/fall times if we assume a 50% duty cycle, that is,  $D = \tau/P = 0.5$ . The magnitudes of the coefficients for odd  $n$  and even  $n$  are

$$|\hat{c}_n| = \frac{A}{2\pi n} \left| \frac{\sin\left(\frac{n\pi\tau_r}{P}\right)}{\frac{n\pi\tau_r}{P}} + \frac{\sin\left(\frac{n\pi\tau_f}{P}\right)}{\frac{n\pi\tau_f}{P}} \right|, \quad n \text{ odd} \quad (1.128a)$$

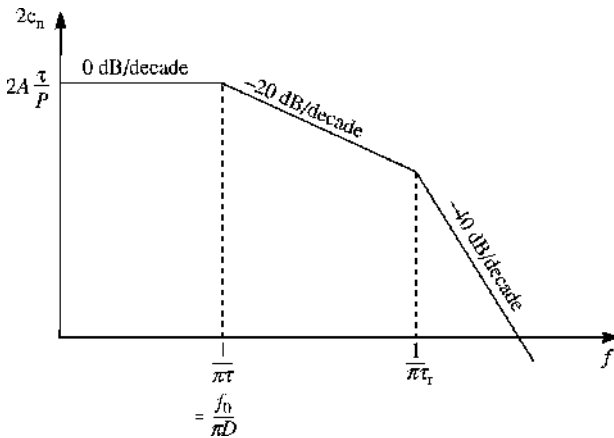


FIGURE 1.23 Spectral bounds for a periodic, trapezoidal pulse train.

and

$$|\hat{c}_n| = \frac{A}{2\pi n} \left| \frac{\sin\left(\frac{n\pi\tau_r}{P}\right)}{\frac{n\pi\tau_r}{P}} - \frac{\sin\left(\frac{n\pi\tau_f}{P}\right)}{\frac{n\pi\tau_f}{P}} \right|, \quad n \text{ even} \quad (1.128b)$$

Observe that for equal rise/fall times, the even harmonics are zero. However, plotting this in asymptotic form as in Figure 1.23 cannot be done since it is not in the form of a product of terms.

The important question of how many harmonics need be included in the sum in (1.121) in order to reasonably reproduce the pulse waveform with that sum can now be estimated for equal rise/fall times. Noting in Figure 1.23 that above the second break point the harmonic amplitudes are rolling off at  $-40$  dB/decade, we might choose to stop the summation at some frequency above this second break point. Since this is a somewhat loose criterion, we might choose for convenience a frequency three times this break frequency. But this is approximately the inverse of the pulse rise time. Hence, we might choose an estimate of the *bandwidth* of a digital pulse as

$$\text{BW} \cong \frac{1}{\tau_r} \quad (1.129)$$

Interestingly, the second  $(\sin x)/x$  function involving the rise/fall time in (1.126) goes to zero at this frequency. In order to illustrate the critical point that addition of each harmonic in time gives a point on the total time-domain waveform and we only need to sum harmonics up to the bandwidth of the pulse in order to obtain a reasonable reproduction of the waveform, we show in Figure 1.24 a 5-V, 100-MHz, 1-ns rise/fall time, 50% duty cycle periodic, trapezoidal pulse train. The bandwidth is, according to (1.129),  $\text{BW} = 1$  GHz. Hence we should sum the first 10 harmonics. The amplitudes and phases of these first 10 harmonics are

$n$	$c_n$	$\angle c_n$ (rad)
1	3.1310	-1.8850
2	0	0
3	-0.9108	-5.6549
4	0	0
5	0.4053	-9.4248
6	0	0
7	-0.1673	-13.1947
8	0	0
9	0.0387	-16.9646
10	0	0

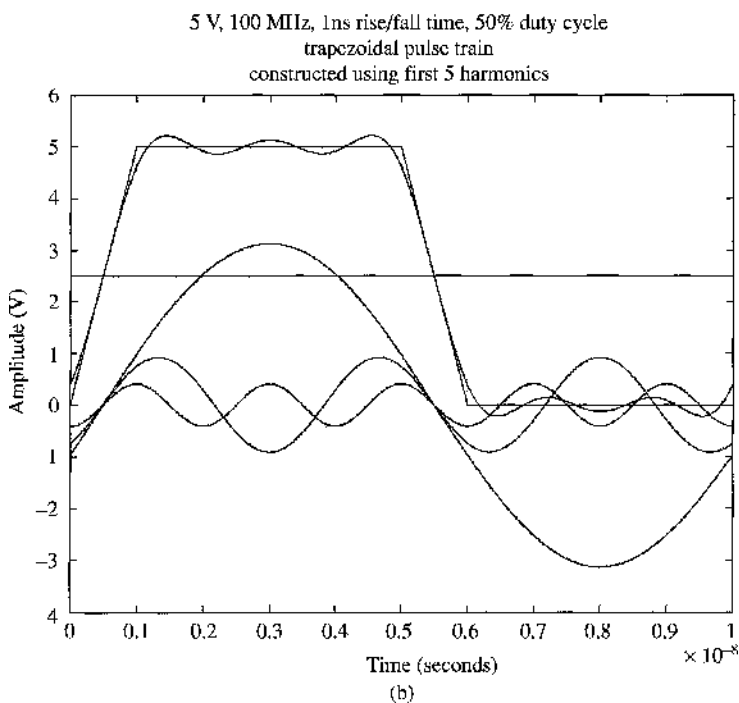
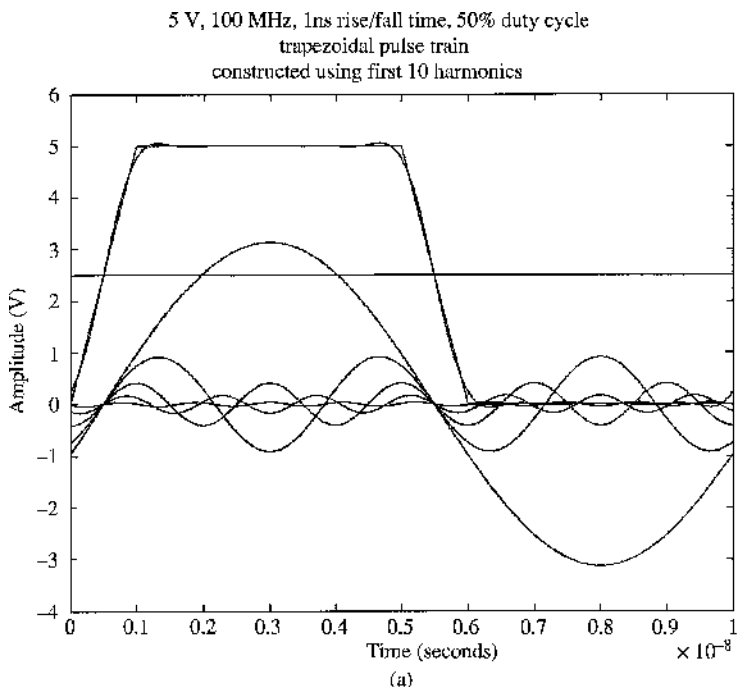


**FIGURE 1.24** Reconstruction of a 5-V, 100-MHz, 1-ns rise/fall time, 50 % duty cycle trapezoidal pulse train (a) using the first 10 harmonics and (b) using the first five harmonics.

Rather than including the minus signs of the third and seventh harmonics in the angle, we have left them in the magnitude. Technically, this is not correct since a magnitude can have no sign, but it simplifies the result. Observe that the even harmonics are zero. This is a characteristic of a 50 % duty cycle waveform. Figure 1.24(a) shows the result of summing the first 10 harmonics. Although there is a small error at the corners, the overall representation is quite good. Figure 1.24(b) shows the result of summing only the first five harmonics. This is another criterion that is often cited for the bandwidth of a digital signal:  $BW = 0.5/\tau_r$ . Observe that the reconstruction with only five harmonics is not so good: there is considerable ringing on the waveform.

### 1.6.3 Computing the Time-Domain Response of Transmission Lines Having Linear Terminations Using Fourier Methods and Superposition

In this section, we will show a very simple but extremely powerful method of solution. It is called the time-domain to frequency-domain or TDFD transformation. A FORTRAN program, TIMEFREQ.FOR, described in Appendix A implements this powerful method. It may also be viewed as a “poor man’s inverse fast Fourier transform (FFT).” The basic idea was described earlier. Decompose the input signal into its sinusoidal harmonic components. Imbed the terminations into a single-input, single-output “black-box” system as illustrated in Figures 1.19 and 1.20. Determine by phasor methods the sinusoidal steady-state response of the transfer function of this single-input, single-output system at each of the harmonics of the input signal. Then pass each sinusoidal component through the system computing the sinusoidal response by phasor methods and sum in time these responses as illustrated in Figure 1.21 to give the time-domain output of the system. Although this gives (within the approximation of a finite number of Fourier components) the time-domain output signal without having to directly solve the differential equations relating the output to the input, there are two important restrictions. (1) In order for this method to be applicable, the system must be *linear* because we have used the principle of *superposition*. For transmission lines, this essentially means that the terminations must be linear because the transmission lines are, in general, linear. For example, if one line is terminated in a diode, then the entire system is nonlinear since this nonlinear termination is imbedded in, and is therefore a part of, the system. (2) This also assumes that the system has reached steady state; that is, the transient portion of the response has decayed to essentially zero. Hence if we apply a periodic waveform to the input as with a digital clock signal, we may have to wait several cycles (periods) or time constants of the system before we will have reached steady state.

As an example of this method, consider the low-pass filter in Figure 1.25(a) consisting of a 1-k $\Omega$  resistor and a 5-pF capacitor. A trapezoidal digital waveform with a frequency of 100 MHz (a period of 10 ns), 5 V amplitude, 50% duty cycle, and 1 ns rise/fall times is applied to the input. Figure 1.25(b) shows the exact output voltage across the capacitor obtained directly in the time domain with PSPICE (see Appendix B for a brief tutorial on the PSPICE program) using the program

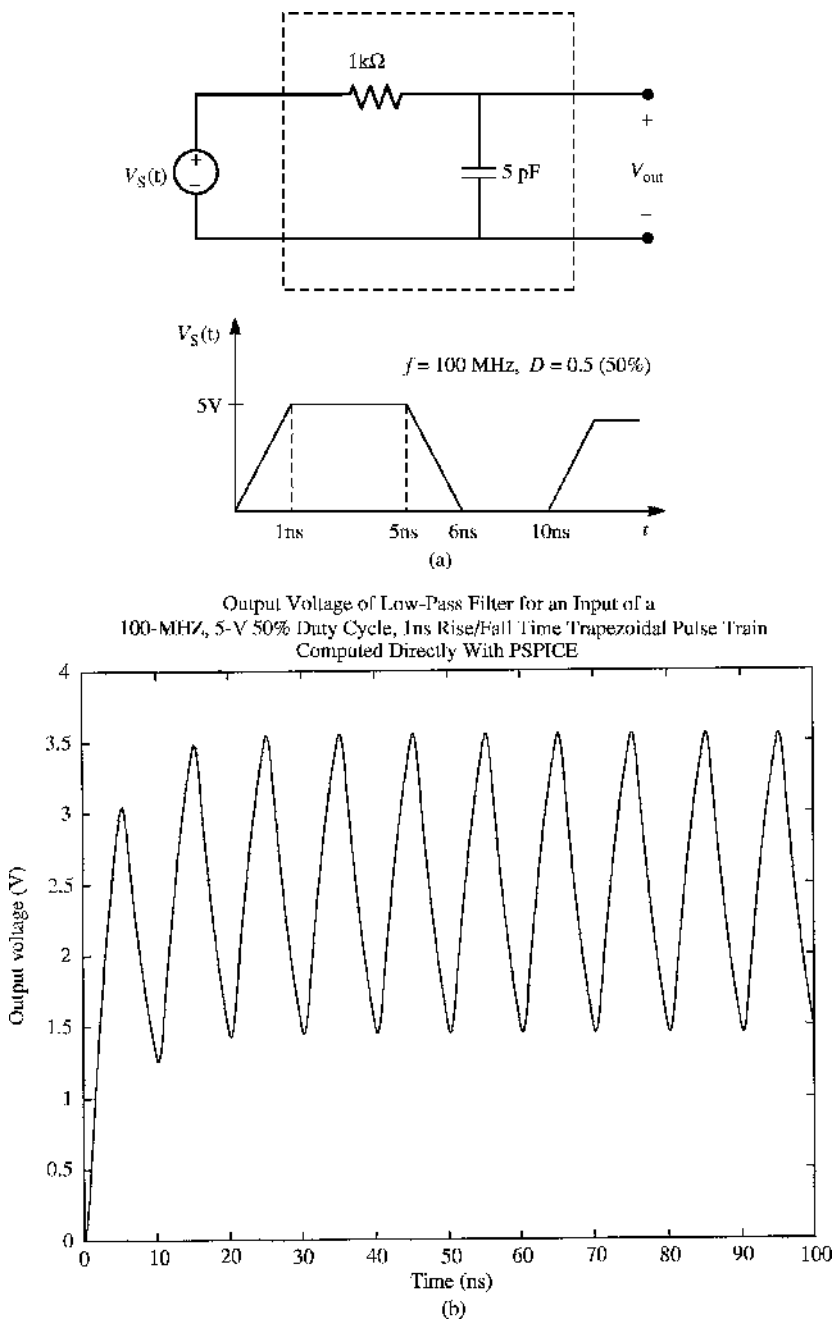


**FIGURE 1.25** An electric circuit example illustrating the use of superposition to combine the responses to harmonics of the input signal: (a) the circuit, (b) the total response computed using PSPICE, and (c) the response by combining the responses to harmonics of the input waveform.

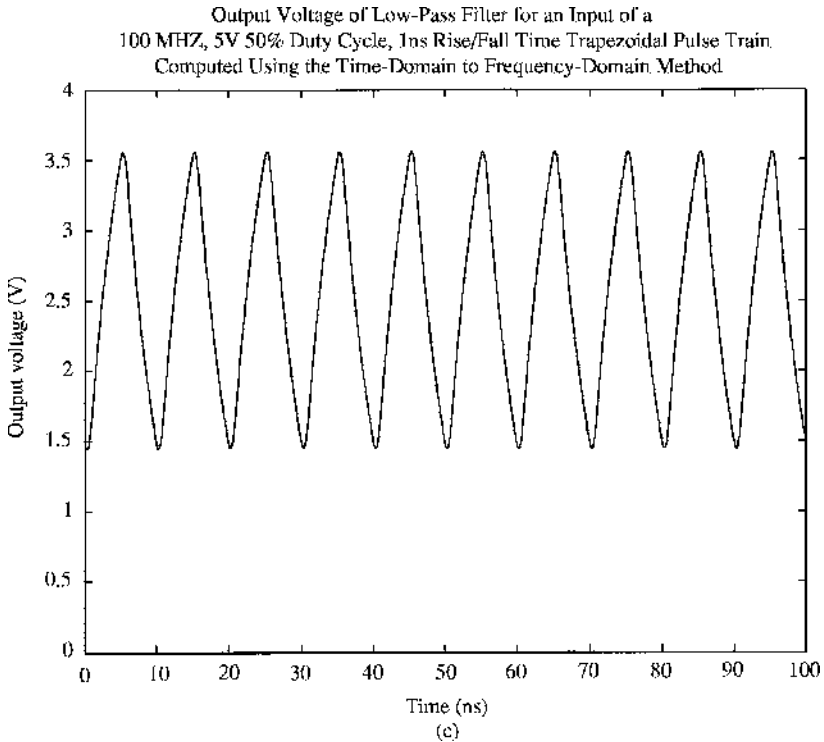


**FIGURE 1.25** (Continued)

**EXAMPLE**

```
VS 1 0 PULSE(0 5 0 1N 1N 4N 10N)
R 1 2 1K
C 2 0 5P
.TRAN 0.1N 100N 0 0.1N
.PROBE
.PRINT TRAN V(2)
.END
```

Observe that there is a transient time interval at the beginning lasting approximately five time constants:  $5RC = 25$  ns. Next, we compute the output using the TDFD method. Since the bandwidth of this signal is on the order of  $BW \cong 1/\tau_r = 1$  GHz, we need to pass frequency components up to 1 GHz through the system. Figure 1.25(c) shows the result of passing the first 10 harmonics, 100 MHz, 200 MHz, 300 MHz, 400 MHz, 500 MHz, 600 MHz, 700 MHz, 800 MHz, 900 MHz and 1 GHz, through the system and summing their responses in time using the TDFD method and the FORTRAN program `TIMEFREQ.FOR`. Observe that this result shows no transient interval; it presupposes that steady state has been reached. Observe also that once the response has reached steady state, the two waveforms are virtually identical.

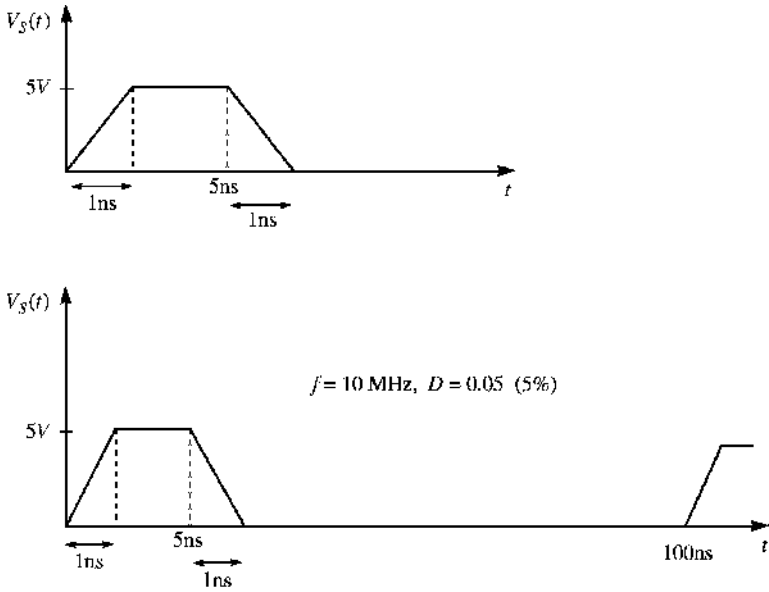
The method can also be used to compute the response to a single pulse. The basic idea is to use a periodic waveform that has the same shape over one period as the desired single pulse *but* choose the period sufficiently long (inverse of the repetition frequency that is chosen sufficiently small) so that the response to the single pulse has essentially reached steady state before the onset of the next pulse in this periodic waveform. For a single pulse that starts at a level of 0 (zero) at  $t = 0$  and ends at a level of 0 at some later time, the steady-state response is also 0. Hence we choose a period that is sufficiently long so that the response has essentially decayed to zero before the onset of the next pulse. For example, suppose we apply a single pulse again having a rise/fall time of 1 ns, a pulse width of 5 ns, and a peak level of 5 V to the low-pass filter in Figure 1.25(a). If we choose the frequency of this periodic waveform long enough, say 100 ns or a frequency of 10 MHz, as shown in Figure 1.26(a), the response will probably have reached steady state before the onset of the next pulse at 100 ns because the time constant of this system is  $RC = 5$  ns. If not, choose a lower frequency. Note that the duty cycle of this new pulse train in Figure 1.26(a) is no longer 50%: it is  $D = 0.05$ . This insures that there is a sufficient length of time after the pulse “turns off” to allow the response to settle down to its steady-state value of 0. Actually, we could choose the duty cycle to be 50% so long as the remaining time after the pulse has turned off, one-half the period, is much longer than the time constant of the system. The exact value of the frequency of this new waveform is not critical; its choice only requires that the system output has reached steady state before the onset of the next pulse in order to use this method to compute the response to a single pulse. The exact time-domain PSPICE simulation (for a single pulse) is obtained with

## EXAMPLE

```
VS 1 0 PWL(0 0 1N 5 5N 5 6N 0)
R 1 2 1K
C 2 0 5P
.TRAN 0.05N 50N 0 0.05N
.PROBE
.PRINT TRAN V(2)
.END
```

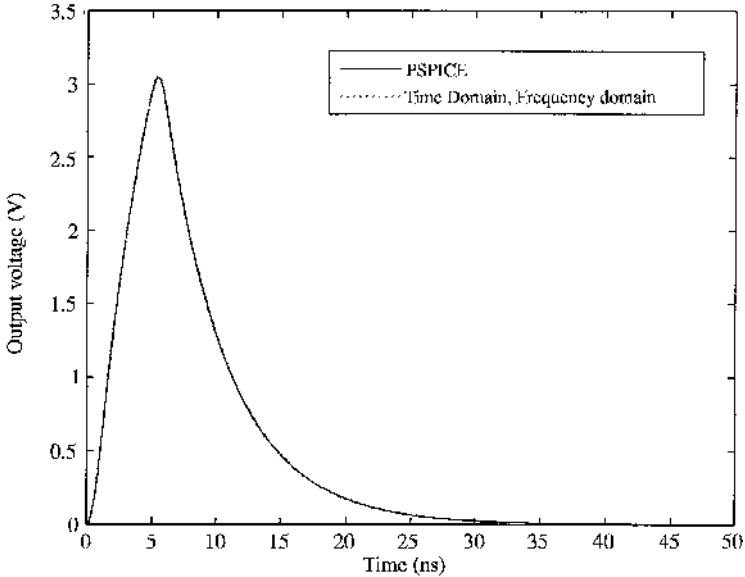
Figure 1.26(b) shows the comparison of the responses of the system to this pulse computed by PSPICE and that computed with the TDFD method using the FORTRAN program TIMEFREQ.FOR (for a 10-MHz pulse train having the same shape as the desired pulse but a duty cycle of  $D = 0.05$  or 5%). The results are virtually identical.

An important advantage of using this method to obtain the time-domain response of a transmission line as opposed to solving the differential equations directly is that losses in the line (in the conductors and the surrounding medium) may be easily incorporated into the frequency-domain transfer function solution and hence into the final solution. The conductor losses above a certain frequency have a  $\sqrt{f}$  dependence due to *skin effect* [1]. This is quite difficult to incorporate into a direct time-domain solution, but it is simple to include in a frequency response calculation. When the terminations are nonlinear, however, we have no choice but to obtain the solution



(a)

Output Voltage of a Low-Pass Filter for a 5V, 5ns pulse width, 1ns Rise/Fall Time Pulse



(b)

**FIGURE 1.26** Illustration of using a periodic waveform with a sufficiently long period to determine the response to a single pulse: (a) the pulse train, (b) computed responses using PSPICE and the TDFD transformation method.

directly in the time domain by solving the differential equations. Frequency-dependent losses then become a very difficult problem to include.

## PROBLEMS

- 1.1** Two perfectly conducting circular plates are separated by a distance  $d$  as shown in Figure P1.1. The plates have very large radii with respect to  $d$  (ideally infinite) so that, in cylindrical coordinates, we may assume a “TEM-mode” field structure,  $\vec{\mathcal{E}}(\rho, t) = \mathcal{E}_z(\rho, t)\vec{a}_z$  and  $\vec{\mathcal{H}}(\rho, t) = \mathcal{H}_\phi(\rho, t)\vec{a}_\phi$ . Define voltage and current as

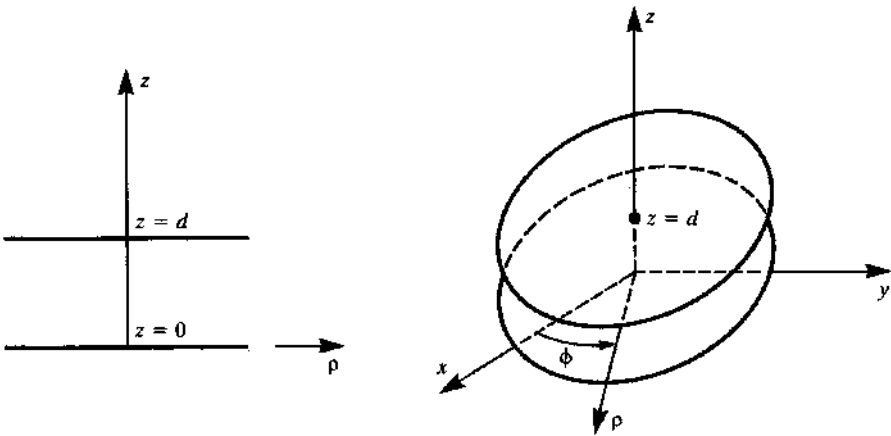


FIGURE P 1.1

$$V(\rho, t) = -\mathcal{E}_z(\rho, t)d$$

$$I(\rho, t) = 2\pi\rho\mathcal{H}_\phi(\rho, t)$$

Show, from Maxwell's equations in cylindrical coordinates, that  $V$  and  $I$  satisfy the transmission-line equations

$$\frac{\partial V(\rho, t)}{\partial \rho} = -l \frac{\partial I(\rho, t)}{\partial t}$$

$$\frac{\partial I(\rho, t)}{\partial \rho} = -c \frac{\partial V(\rho, t)}{\partial t}$$

where  $l$  and  $c$  are static parameters defined by

$$l = \frac{\mu d}{2\pi\rho}$$

$$c = \frac{2\pi\varepsilon\rho}{d}$$

Would it be appropriate to classify this as a *nonuniform* line? Could the mode of propagation to which these equations apply be classified as a “TEM mode”?

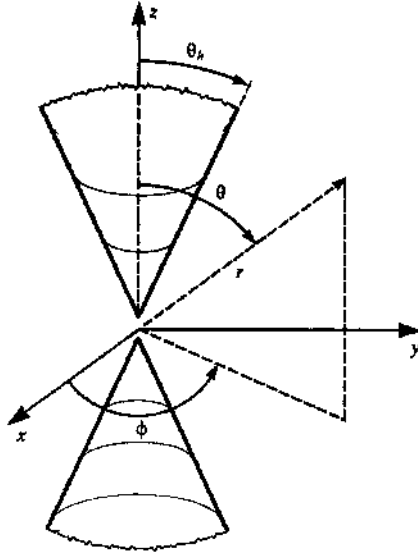


FIGURE P1.2

- 1.2 The infinite biconical transmission line consists of two perfectly conducting cones of half angle  $\theta_h$  as shown in Figure P1.2. Solve Maxwell's equations in spherical coordinates for this structure assuming that  $\vec{\mathcal{E}}(r, \theta) = \mathcal{E}_\theta(r, \theta)\vec{a}_\theta$  and  $\vec{\mathcal{H}}(r, \theta) = \mathcal{H}_\phi(r, \theta)\vec{a}_\phi$ . Show that the following definitions of voltage and current are unique:

$$V(r, t) = \int_{\theta_h}^{\pi - \theta_h} \mathcal{E}_\theta r d\theta$$

$$I(r, t) = \int_0^{2\pi} \mathcal{H}_\phi r \sin(\theta) d\phi$$

where  $V$  and  $I$  satisfy the following transmission-line equations:

$$\frac{\partial V(r, t)}{\partial r} = -l \frac{\partial I(r, t)}{\partial t}$$

$$\frac{\partial I(r, t)}{\partial r} = -c \frac{\partial V(r, t)}{\partial t}$$

Show that

$$l = \frac{\mu}{\pi} \ln \left( \cot \frac{\theta_h}{2} \right)$$

$$c = \frac{\pi \epsilon}{\ln \left( \cot \frac{\theta_h}{2} \right)}$$

Would this be classified as a *uniform* or *nonuniform* line? Would it be appropriate to classify the propagation mode as TEM?

- 1.3 Show that, assuming a TEM field structure, the currents on the two conductors in Figure 1.5 are equal in magnitude and oppositely directed at any cross section.
- 1.4 Show that, assuming a TEM field structure, the charge per unit length on one conductor in Figure 1.5 is equal in magnitude and opposite in sign to the charge per unit length on the other conductor at any cross section.
- 1.5 Consider the coaxial cable in Figure 1.1(c) consisting of an exterior shield and an inner wire that is located on the axis of the shield. The dielectric interior to the shield has a relative permittivity of  $\epsilon_r = 2.3$ . Determine the velocity of propagation and the one-way time delay on the line,  $T_D = \mathcal{L}/v$ , for a line of total length  $\mathcal{L} = 10$  m. [50.55 ns]

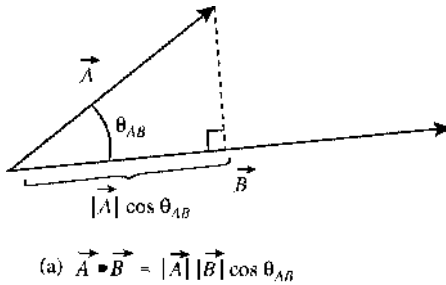


FIGURE P 1.7

- 1.6 Consider the stripline in Figure 1.2(a) consisting of one land between two infinite ground planes. The dielectric is glass epoxy with  $\epsilon_r = 4.7$ . Determine the velocity of propagation and the one-way time delay on the line,  $T_D = \mathcal{L}/v$ , for a line of total length  $\mathcal{L} = 10$  in. [1.84 ns]
- 1.7 The *dot product* of two vectors is defined as  $\vec{A} \cdot \vec{B} = |\vec{A}| |\vec{B}| \cos \theta_{AB}$ , where  $|\vec{A}|$  denotes the magnitude (length) of vector  $\vec{A}$  [A.1]. The dot product can be thought of as the product of the length of one vector and the projection of the other vector on this vector as illustrated in Figure P1.7. The dot product gives a *scalar* as the result. The dot product can be mechanically computed from  $\vec{A} \cdot \vec{B} = A_x B_x + A_y B_y + A_z B_z$  [A.1]. For the two vectors  $\vec{A} = 3\vec{a}_x + 2\vec{a}_y$  and

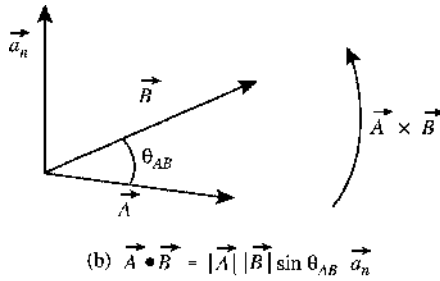


FIGURE P1.8

$\vec{B} = 2\vec{a}_x - 5\vec{a}_y$ , determine the dot product of the two vectors (a) directly and (b) using the basic definition of the dot product. Repeat for  $\vec{A} = 2\vec{a}_x - 3\vec{a}_y$  and  $\vec{B} = 5\vec{a}_x$ . [-4, 10]

- 1.8** The *cross product* of two vectors is defined as  $\vec{A} \times \vec{B} = |\vec{A}| |\vec{B}| \sin \theta_{AB} \vec{a}_n$ , where  $|\vec{A}|$  denotes the magnitude (length) of vector  $\vec{A}$  and  $\vec{a}_n$  is a unit vector normal or perpendicular to the plane containing the vectors  $\vec{A}$  and  $\vec{B}$  [A.1]. There are two sides to this plane, so the unit vector  $\vec{a}_n$  direction is determined according to the *right-hand rule* as illustrated in Fig. P1.8. The cross product gives a *vector* as the result. The cross product can be mechanically computed from [A.1]

$$\vec{A} \times \vec{B} = (A_y B_z - A_z B_y) \vec{a}_x + (A_z B_x - A_x B_z) \vec{a}_y + (A_x B_y - A_y B_x) \vec{a}_z$$

For the vectors  $\vec{A} = \vec{a}_z$  and  $\vec{B} = E\vec{a}_x$ , determine the cross product (a) directly and (b) from the basic definition of the cross product. (Set up a rectangular coordinate system and use your right hand.) Repeat this for  $\vec{A} = \vec{a}_x$  and  $\vec{B} = E\vec{a}_z$  and  $\vec{A} = \vec{a}_y - \vec{a}_z$  and  $\vec{B} = E\vec{a}_x$ . [ $E\vec{a}_y, -E\vec{a}_y, -E\vec{a}_y, -E\vec{a}_z$ ]

- 1.9** The *divergence* of a vector field is given by [A.1]

$$\nabla \cdot \vec{\mathcal{E}}(x, y, z) = \frac{\partial \mathcal{E}_x}{\partial x} + \frac{\partial \mathcal{E}_y}{\partial y} + \frac{\partial \mathcal{E}_z}{\partial z}$$

The divergence of a vector field gives the net *outflow* of the vector field from a point and hence locates sources and sinks of the vector field. Determine the divergence of  $\vec{\mathcal{E}} = E_0 \vec{a}_x$ . Repeat for  $\vec{\mathcal{E}} = x\vec{a}_x + y\vec{a}_y$ . Interpret these results. [0,  $x + y$ ]

- 1.10** The *curl* of a vector field in rectangular coordinates is given by [A.1]

$$\nabla \times \vec{\mathcal{E}} = \left( \frac{\partial \mathcal{E}_z}{\partial y} - \frac{\partial \mathcal{E}_y}{\partial z} \right) \vec{a}_x + \left( \frac{\partial \mathcal{E}_x}{\partial z} - \frac{\partial \mathcal{E}_z}{\partial x} \right) \vec{a}_y + \left( \frac{\partial \mathcal{E}_y}{\partial x} - \frac{\partial \mathcal{E}_x}{\partial y} \right) \vec{a}_z$$

The curl gives the net circulation of the field much like vortices or eddies in a river. Determine the curl of  $\vec{\mathcal{E}} = E_0\vec{a}_y$ . Repeat for  $\vec{\mathcal{E}} = -y\vec{a}_x + x\vec{a}_y$ . Interpret these results.  $[0, 2\vec{a}_z]$

**1.11** Demonstrate that the various components in (1.3) are in the indicated directions. (Draw a rectangular coordinate system and use your right hand.)

**1.12** Demonstrate the identity in (1.5), where the gradient is defined as [A.1]

$$\nabla f(x, y, z) = \frac{\partial f}{\partial x}\vec{a}_x + \frac{\partial f}{\partial y}\vec{a}_y + \frac{\partial f}{\partial z}\vec{a}_z$$

**1.13** Demonstrate the identity in (1.11).

**1.14** Demonstrate the result in (1.13).

**1.15** Show that the general solutions in (1.16) satisfy the equations in (1.15).

**1.16** Power flow in an electromagnetic field is given by the Poynting vector [A.1] as

$$\vec{S} = \vec{\mathcal{E}} \times \vec{\mathcal{H}}$$

Show that the forward- and backward-traveling waves in (1.20) give the proper direction of power flow. (Draw a rectangular coordinate system and use your right hand.)

**1.17** Show that (1.25) satisfy the phasor differential equations in (1.24).

**1.18** Show that (1.34) satisfy the phasor differential equations in (1.32).

**1.19** Show that the voltage definition in (1.40) reduces as shown.

**1.20** Derive the transmission-line equations from each of the circuits in Figure P1.20 in the limit as  $\Delta z \rightarrow 0$ . Observe that the total inductance (capacitance) in each structure is  $l\Delta z(c\Delta z)$ . This shows that the structure of the per-unit-length equivalent circuit is not important in obtaining the transmission-line equations from it so long as the total per-unit-length inductance and capacitance is contained in the structure and we let  $\Delta z \rightarrow 0$ .

**1.21** Demonstrate the identities in (1.65) and (1.69).

**1.22** Derive the second-order transmission-line equations in (1.72).

**1.23** A coaxial cable shown in Figure P1.23 has an interior dielectric that is defined in annuli as  $\varepsilon_1, \mu_0$  for  $r_w < r < a$  and  $\varepsilon_2, \mu_0$  for  $a < r < r_s$ . Is this a uniform transmission line? Is the medium homogeneous or inhomogeneous? How would you compute the per-unit-length capacitance for this transmission line? (Recall that capacitors in series add like resistors in parallel and capacitors in parallel add like resistors in series.)

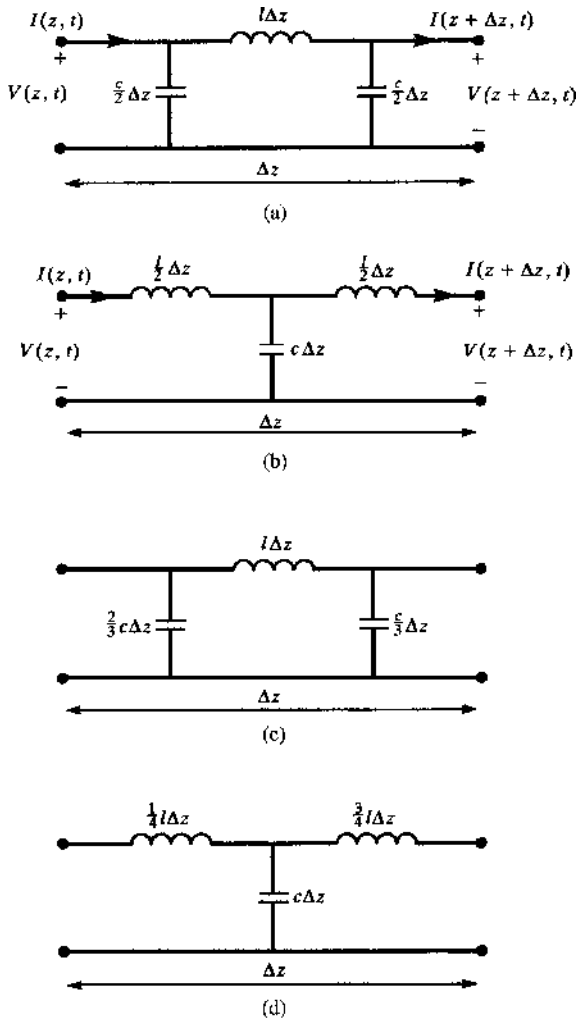


FIGURE P 1.20

- 1.24 A stripline shown in Figure P1.24 has a dielectric that is defined in planes of thickness  $a$  and  $b$  as  $\epsilon_1, \mu_0$  and  $\epsilon_2, \mu_0$ . Is this a uniform transmission line? Is the medium homogeneous or inhomogeneous? How would you compute the per-unit-length capacitance for this transmission line? (Recall that capacitors in series add like resistors in parallel, and capacitors in parallel add like resistors in series.)
- 1.25 Demonstrate the relations in (1.81) and (1.85).
- 1.26 Demonstrate the relations in (1.87).

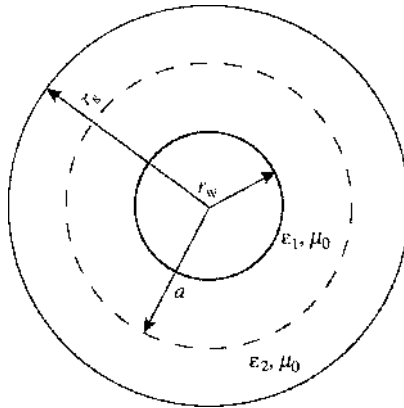


FIGURE P 1.23

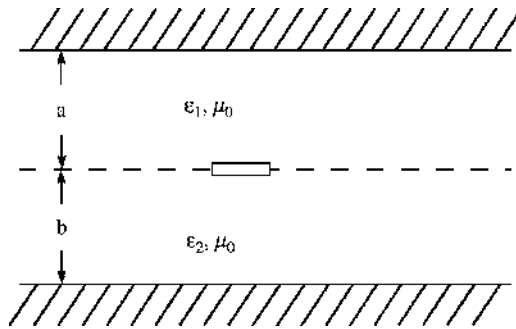


FIGURE P 1.24

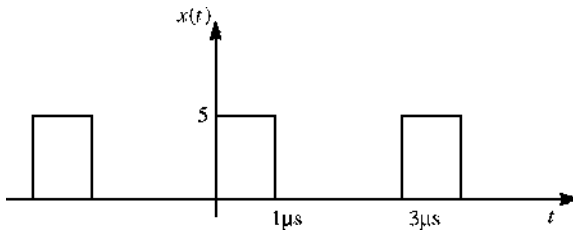


FIGURE P 1.28

- 1.27 Demonstrate the per-unit-length parameters of the parallel-plate line in (1.102).
- 1.28 Determine the Fourier coefficients in (1.122) for the square-wave waveform in Figure P1.28. [ $\hat{c}_n = (5/3)(\sin(n\pi/3))/(n\pi/3) \angle -n\pi/3$ ].
- 1.29 Determine the Fourier coefficients in (1.122) for the full-wave rectified waveform in Figure P1.29. [ $\hat{c}_n = (2A/\pi(1 - 4n^2))$ ]

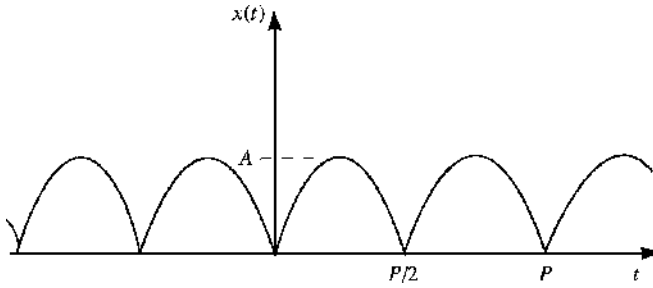


FIGURE P 1.29

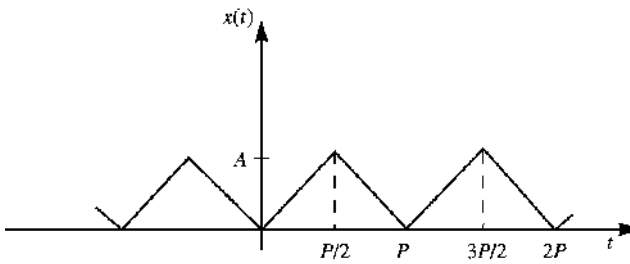


FIGURE P 1.30

- 1.30** Determine the Fourier coefficients in (1.122) for the triangular waveform in Figure P1.30. [ $c_0 = (A/2)$ ,  $\hat{c}_n = -(2A/(n\pi)^2)$   $n$  odd]
- 1.31** Use MATLAB or PSPICE to recombine the first 10 harmonics of the waveform in Figure P1.28 to give an approximation to the time-domain waveform.

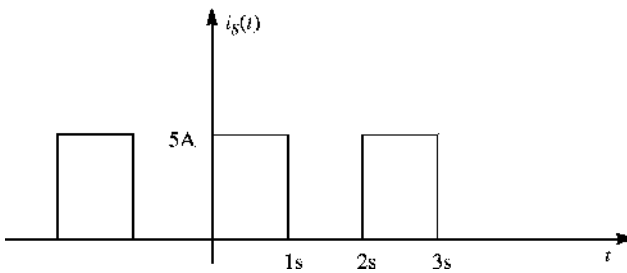
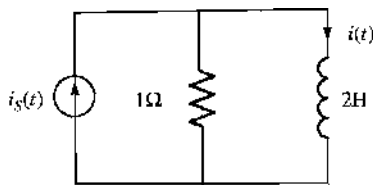


FIGURE P 1.34

- 1.32** Use MATLAB or PSPICE to recombine the first 10 harmonics of the waveform in Figure P1.29 to give an approximation to the time-domain waveform.
- 1.33** Use MATLAB or PSPICE to recombine the first 10 harmonics of the waveform in Figure P1.30 to give an approximation to the time-domain waveform.
- 1.34** The square-wave current source in Figure P1.34 is applied to the associated circuit as shown. Determine the resulting output current through the inductor,  $i(t)$ , in the form

$$i(t) = I_0 + \sum_{n=1}^7 I_n \cos(n\omega_0 t + \theta_n)$$

Use PSPICE and TIMEFREQ.FOR to determine the output current of this linear system and compare the approximation using a finite number of Fourier components (seven for TIMEFREQ.FOR) to the exact result (using PSPICE). [ $I_0 = 2.5$ ,  $I_1 = 0.5$ ,  $\theta_1 = -80.96^\circ$ ,  $I_2 = 0$ ,  $I_3 = 0.0562$ ,  $\theta_3 = -86.96^\circ$ ,  $I_4 = 0$ ,  $I_5 = 0.0203$ ,  $\theta_5 = -88.17^\circ$ ,  $I_6 = 0$ ,  $I_7 = 0.0103$ ,  $\theta_7 = -88.7^\circ$ ]

## REFERENCES

- [1] S. Ramo, J.R. Whinnery, and T. VanDuzer, *Fields and Waves in Communication Electronics*, 2nd edition, John Wiley & Sons, New York, 1984.
- [2] R.B. Adler, L.J. Chu, and R.M. Fano, *Electromagnetic Energy Transmission and Radiation*, John Wiley, New York, 1963.
- [3] S. Frankel, *Multiconductor Transmission Line Analysis*, Artech House, Dedham, MA, 1977.
- [4] H. Uchida, *Fundamentals of Coupled Lines and Multiwire Antennas*, Sasaki Publishing Co, Sendai, Japan, 1967.
- [5] S. Hayashi, *Surges on Transmission Systems*, Denki-Shoin, Kyoto, Japan, 1955.
- [6] W.C. Johnson, *Transmission Lines and Networks*, McGraw-Hill, New York, 1950.
- [7] L.V. Bewley, *Traveling Waves on Transmission Systems*, 2nd edition, John Wiley & Sons, New York, 1951.
- [8] P.I. Kuznetsov and R.L. Stratonovich, *The Propagation of Electromagnetic Waves in Multiconductor Transmission Lines*, Macmillan, New York, 1964.
- [9] P.C. Magnuson, *Transmission Lines and Wave Propagation*, Allyn & Bacon, Newton, MA, 1970.
- [10] R.E. Collin, *Field Theory of Guided Waves*, 2nd edition, IEEE Press, New York, 1991.
- [11] J. Zaborsky and J.W. Rittenhouse, *Electric Power Transmission*, Ronald Press, New York, 1954.
- [12] R.E. Matlick, *Transmission Lines for Digital and Communication Networks*, McGraw-Hill, New York, 1969.

- [13] L. Young (ed.), *Parallel Coupled Lines and Directional Couplers*, Artech House, Dedham, MA, 1972.
- [14] T. Itoh (ed.), *Planar Transmission Line Structures*, IEEE Press, New York, 1987.
- [15] W.T. Weeks, Multiconductor transmission line theory in the TEM approximation, *IBM Journal of Research and Development*, 604–611, 1972.
- [16] K.D. Marx, Propagation modes, equivalent circuits and characteristic terminations for multiconductor transmission lines with inhomogeneous dielectrics, *IEEE Transactions on Microwave Theory and Techniques*, **21**, 450–457, 1973.
- [17] A.F. dos Santos and J.P. Figanier, The method of series expansion in the frequency domain applied to multiconductor transmission lines, *IEEE Transactions on Microwave Theory and Techniques*, **23**(9), 753–756, 1975.
- [18] I.V. Lindell, On the quasi-TEM modes in inhomogeneous multiconductor transmission lines, *IEEE Transactions on Microwave Theory and Techniques*, **29**(8), 812–817, 1981.
- [19] Y. Leviatan and A.T. Adams, The response of a two-wire transmission line to incident field and voltage excitation, including the effects of higher order modes, *IEEE Transactions on Antennas and Propagation*, **30**(5), 998–1003, 1982.
- [20] K.S.H. Lee, Two parallel terminated conductors in external fields, *IEEE Transactions on Electromagnetic Compatibility*, **20**, 288–295, 1978.
- [21] S. Frankel, Forcing functions for externally excited transmission lines, *IEEE Transactions on Electromagnetic Compatibility*, **22**, 210, 1980.
- [22] C.R. Paul and D.R. Bush, Radiated emissions from common-mode currents, *Proceedings of the 1987 IEEE International Symposium on Electromagnetic Compatibility*, Atlanta, GA, (September 1987).
- [23] C.R. Paul, A comparison of the contributions of common-mode and differential-mode currents in radiated emissions, *IEEE Transactions on Electromagnetic Compatibility*, **31**, 189–193, 1989.
- [24] K.B. Hardin, Decomposition of radiating structures to directly predict asymmetric-mode radiation, PhD dissertation, University of Kentucky, 1991.